Final Report

ENHANCED MOLECULAR SIEVE CO$_2$ REMOVAL EVALUATION

97-69288
September 5, 1997

Prepared for

**NASA Headquarters
Washington, D.C.**

Contract NASW-5033

△llliedSignal Aerospace Equipment Systems
Torrance
A E R O S P A C E

FOREWORD

This report, submitted by AlliedSignal Aerospace Equipment Systems, Torrance, CA, documents and summarizes the results of the work completed during the two-year Enhanced Molecular Sieve CO_2 Removal Program under NRA Contract NASW-5033. The objective of this two-year research program was to quantitatively characterize the performance of two major types of molecular sieves for two-bed regenerative CO_2 removal systems at conditions compatible with future EVA and IVA missions.

CONTENTS

CONTENTS (Continued)

ILLUSTRATIONS

ILLUSTRATIONS (Continued)

TABLES

1. PROJECT DESCRIPTION

1.1 OBJECTIVE

This research program is concerned with the laboratory evaluation of two different types of CO_2 removal adsorbents: (1) zeolite molecular sieves and (2) carbon molecular sieves (CMS). Both types of molecular sieves will enable the development of two-bed regenerable CO_2 removal systems for long-duration station-type applications and for portable life support systems (PLSS) in extravehicular and intravehicular activity (EVA and IVA) applications. The objective of this project is to quantitatively characterize the performance of these sorbents in a cycling pressure-swing system. The results will establish comparative advantages of these adsorbents and provide a database upon which future systems can be developed.

The two-bed regenerable molecular sieve system (Figure 1-1) provides a simple means of removing CO_2 for air revitalization. The system comprises two (adsorbent) beds and associated valves and actuators. The beds alternately adsorb and desorb metabolically generated carbon dioxide to remove it from the air and vent it overboard. After a bed has adsorbed carbon dioxide, the bed is adiabatically regenerated (desorbed) via exposure to space vacuum. The adsorbed carbon dioxide and a small amount of air are lost to vacuum during the regeneration.
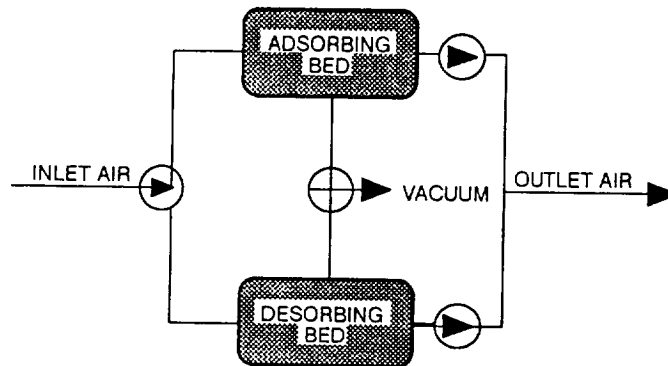
IG-18321-1A

Figure 1-1. Two-Bed Regenerable Molecular Sieve CO_2 Removal System

Because of their removal efficiency and low power consumption, pressure swing CO_2 adsorption systems have been used for a number of space environmental control systems, including Skylab, the Space Shuttle Extended Duration Orbitor, and the Space Station carbon dioxide removal assembly (CDRA).

1.2 TECHNICAL REQUIREMENTS

CO_2 removal requirements representative of those for the International Space Station ECLSS design loads (four people) and a portable life support system for extravehicular activity (one person) are shown in Table 1-1. These requirements were used to establish the range of test conditions for this research program.

TABLE 1-1

CO₂ REMOVAL TECHNICAL REQUIREMENTS

Parameter	International Space Station ECLSS	Portable Life Support System
Metabolic CO_2 production, kg/hr	0.18 to 0.21	0.09
CO_2 partial pressure, kPa	0.4	1.0
O_2 partial pressure, kPa	19 to 22	23
Total pressure, kPa	101	57.2
Temperature, K	291 to 297	291 to 305
Dewpoint, K	278 to 289	289 to 301
Relative humidity, percent	25 to 70	40 to 100

1.2.1 Sorbent Selection

Two major types of CO_2 adsorbents were selected for characterization:

(a) Zeolite-based molecular sieves 13X and 5A. The 5A material has been further processed by AlliedSignal to enhance the CO_2 capacity. Equal volumetric portions of Type 13X for moisture removal and Type 5A for CO_2 removal were selected as the baseline bed. This composition is similar to the CDRA adsorbent beds.

(b) Carbon molecular sieve, which has been functionalized to improve its capacity to adsorb carbon dioxide.

Additional details on the physical properties of the sorbents are presented in Section 2.

1.2.2 Flow Rate

Mass transfer, or the amount of CO_2 adsorbed by the bed, is proportional to the residence time of the airflow in the adsorption bed. Space velocity is an expression of the airflow rate in terms of the number of bed volumes per second, which is the reciprocal of the residence time. For station tests, the design point space velocity of the space station carbon dioxide removal assembly (CDRA) was used. For suit tests, the flow rates were varied around a baseline of a 0.5-sec residence time.

1.2.3 CO₂ Concentration

The difference in the CO_2 partial pressure between the airflow and the sorbent is the driving force for adsorption. In static testing, it is not necessary to test at the total pressure used in the application as long as the CO_2 partial pressure is equivalent. Dynamic adsorption tests were conducted at 1.0-atm total pressure, with the inlet CO_2 partial pressure of 2 mm or 4 mm Hg partial pressure CO_2 for space station application and at 3.75-psia total pressure and 6 mm Hg partial pressure CO_2 representative of a PLSS application.

1.2.4 Moisture Content

The relative humidity in the inlet air stream can vary from 25 to 100 percent. Relative humidity greater than 80 percent was used for all tests presented in this report unless otherwise noted.

1.2.5 Thermal Conditions

Sorbents liberate heat on adsorption and absorb heat on desorption. As indicated by the equilibrium characteristics, the sorbent adsorbs less at higher temperature and desorbs better at higher temperatures.

Tests were performed under adiabatic, thermally coupled, and isothermal conditions. The transient temperature behavior of the sorbent beds was recorded to provide a basis for understanding the impact and effectiveness on the overall absorption/ desorption performance due to thermal coupling.

1.3 TECHNICAL ACHIEVEMENTS

Key results obtained on this program include the following:

- Pressure-swing CO_2 removal systems appear competitive with existing CO_2 removal system for both suit and station applications.

- The isothermal and thermally coupled beds show similar performance, and both are superior to the performance obtained in the adiabatic bed

- FCMS can be completely regenerated in a pressure-swing system; zeolites were unable to be completely regenerated without the addition of heat.

- FCMS shows repeatable and stable performance in a cycling pressure-swing system.

- FCMS sorbents can be fabricated to adsorb CO_2 independently of the humidity in the air. This fabrication process is repeatable and shows consistent capacities.

- No degradation in material performance was observed over the duration of this test program.

2. MATERIAL CHARACTERIZATION

Design data for the Type 5A and 13X zeolite materials were developed earlier by AlliedSignal and the results presented in NASA CR-2277, "Development of Design Information for Molecular-Sieve Type Regenerative CO_2 Removal Systems". Equilibrium properties for CO_2 and moisture adsorption for each of the zeolites were established, including equilibrium data for the coadsorption of water and CO_2.

Recent tests have established the equilibrium behavior of the enhanced 5A zeolite and the new functionalized carbon molecular sieves. The equilibrium isotherms that define the maximum capacity of the molecular sieves and other basic data are presented in this section.

2.1 ZEOLITE

The selected zeolite-based molecular sieves, 5A and 13X, are used on the Space Station carbon dioxide removal assembly (CDRA) and represent the best current technology. Both of these adsorbents exhibit selective adsorption of CO_2, although they are also hydrophilic, especially the 13X. Water adsorption significantly degrades the molecular sieve capacity for CO_2 adsorption, as shown in Figure 2-1 (NASA-CR-2277). The adsorption bed design approach is to locate the 13X material upstream, where it removes the majority of the moisture present in the air stream before it contacts the 5A material, thereby enabling the 5A to retain its full CO_2 removal capacity. A photograph of this 5A sieve is shown in Figure 2-2. The CO_2 adsorption isotherm of the advanced 5A produced is illustrated in Figure 2-3 for comparison with a commercial Grace 5A.
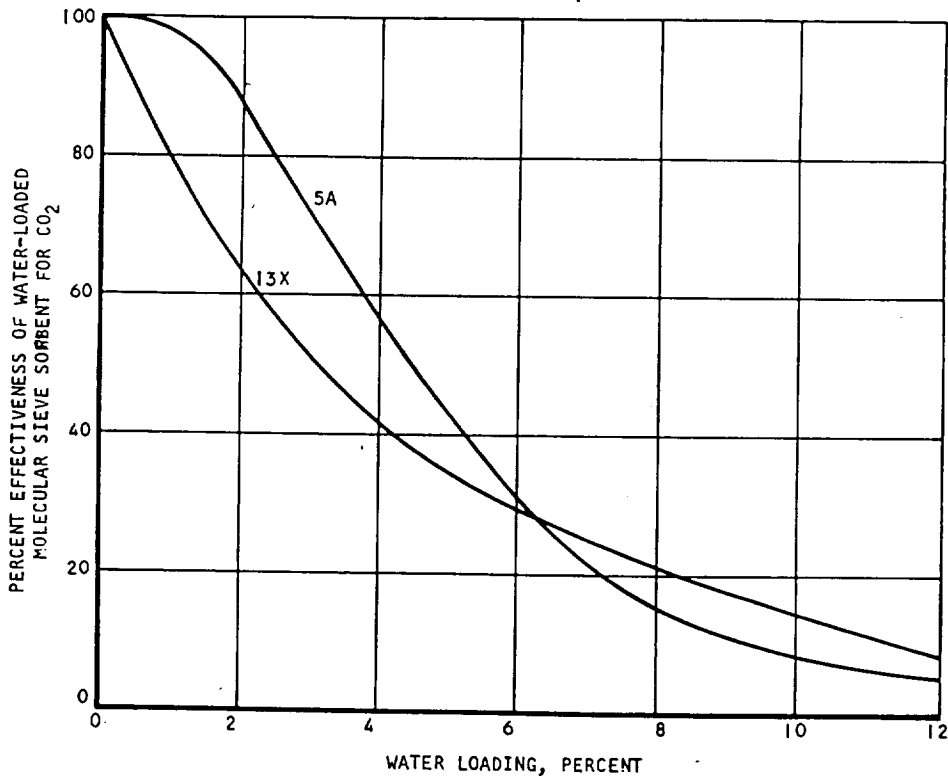
S-66220

Figure 2-1. Effectiveness of Water-Loaded Zeolite Molecular Sieve Sorbent for CO_2
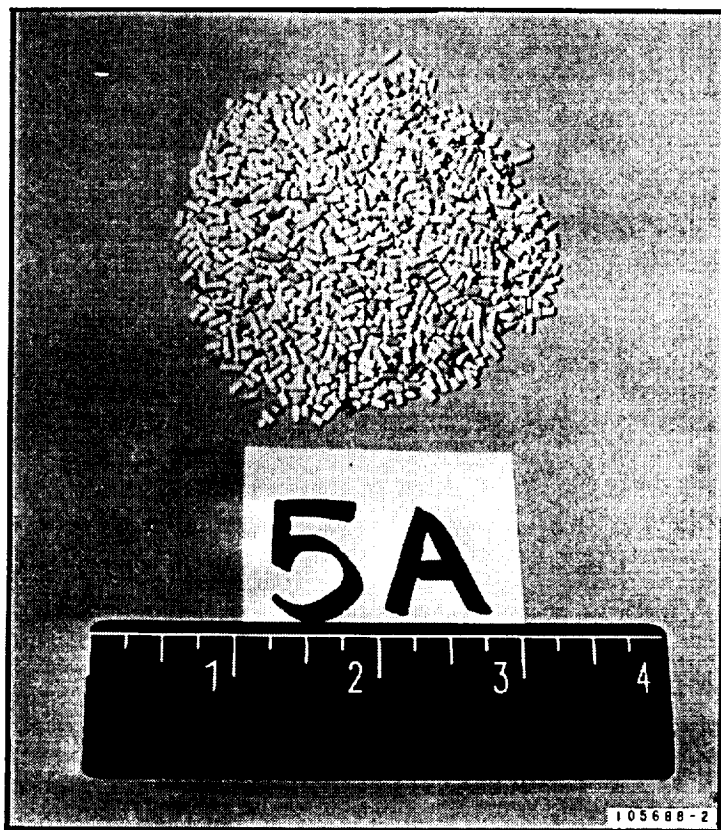
Figure 2-2. Advanced 5A Sieve (Photograph)
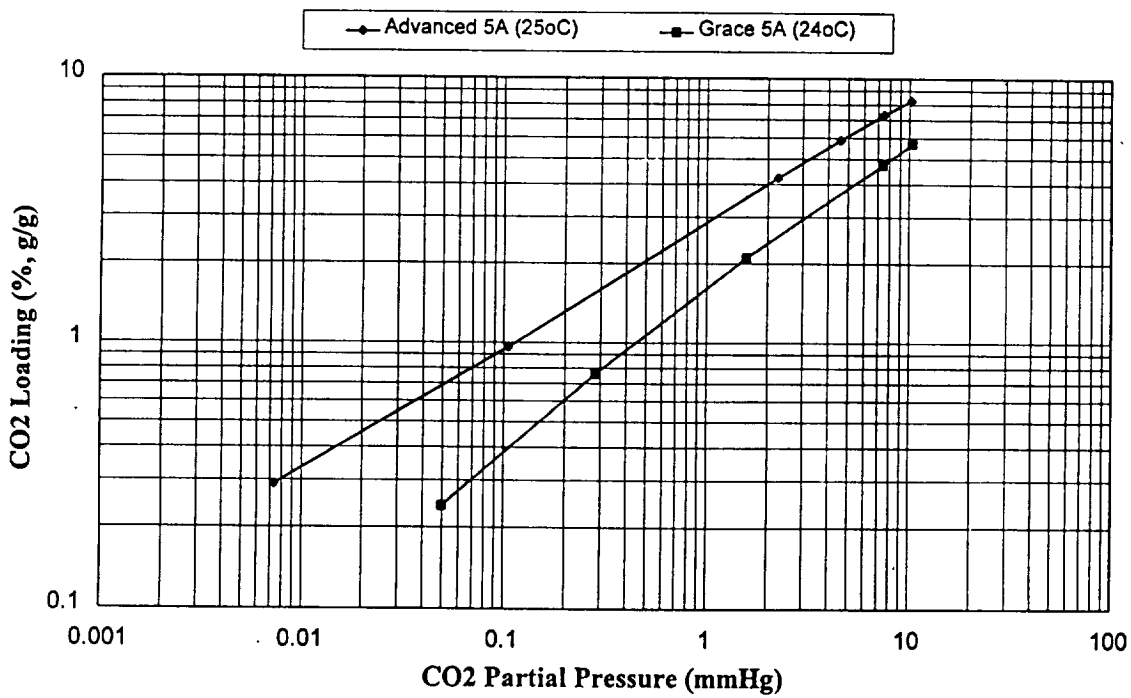
Figure 2-3. CO$_2$ Isotherms on 5A at 25°C

AlliedSignal
AEROSPACE
Aerospace Equipment Systems
Torrance

97-69288
Page 2-2

AlliedSignal developed an advanced version of the 5A material, which exhibits superior CO_2 capacity. The version being characterized in this program is similar to the CDRA material. The CO_2 adsorption isotherms obtained for the advanced 5A are shown in Figure 2-4 for various temperatures.

Carbon dioxide and water adsorption isotherms for the 13X material are presented in Figures 2-5 and 2-6 (NASA-CR-2277), respectively. The material can adsorb up to 26 percent water by weight when exposed to a 50 percent relative humidity laboratory ambient condition. A photograph of the 13X material used in the test program is shown in Figure 2-7.

The performance of the zeolites in a space application is limited by the characteristic that the adsorbent is hydrophilic and takes up water vapor in preference to carbon dioxide. As the adsorbent picks up water, the capacity for carbon dioxide degrades. For this reason, conventional systems utilize a separate desiccant bed to remove water vapor upstream of the CO_2 removal bed.

2.2 CARBON MOLECULAR SIEVE (CMS)

Carbon molecular sieves can be used in a number of gas separation processes because of their unique properties. AlliedSignal has developed a CMS with a large surface area, greater than 1000 m^2/gram, and a uniform pore size distribution. By
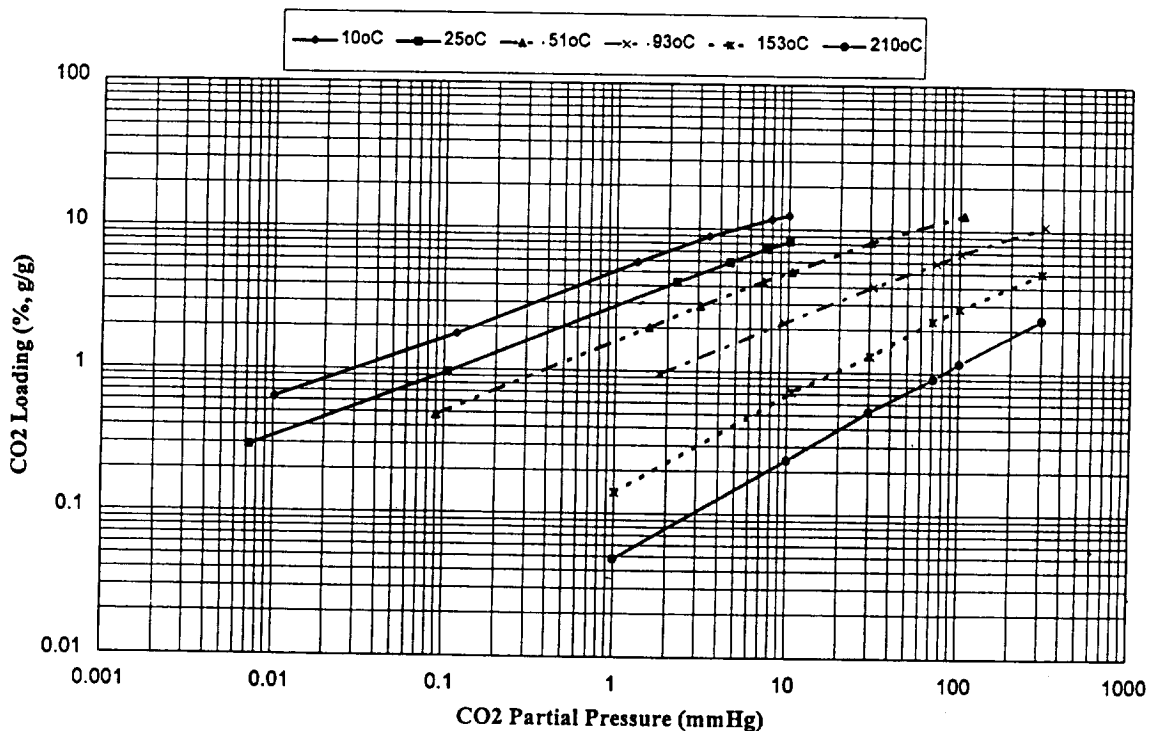
Figure 2-4. CO_2 Adsorption Isotherms on Advanced 5A Zeolite
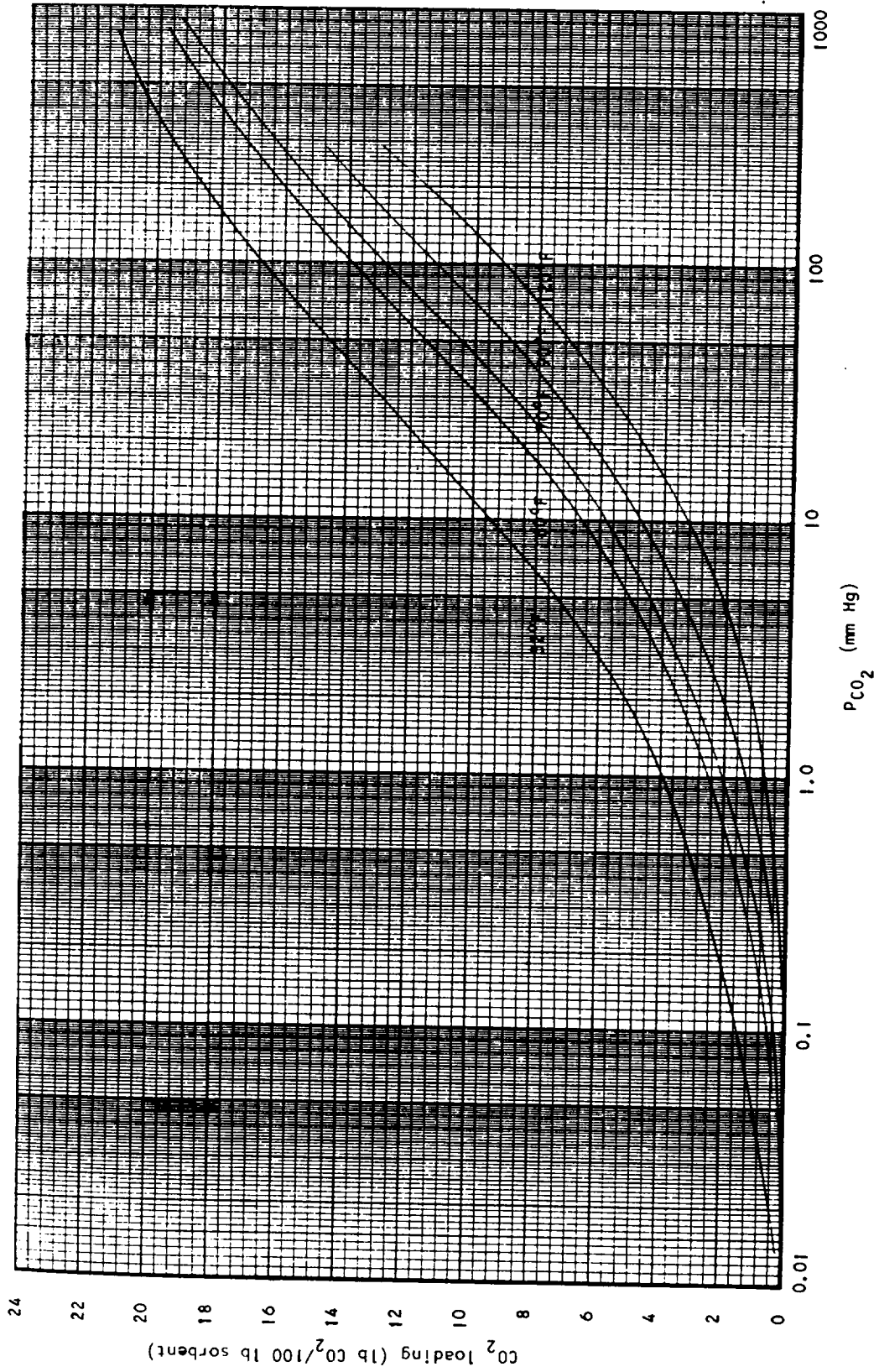
Figure 2-5. Carbon Dioxide Equilibrium Data for Linde 13X Sorbent

AlliedSignal
AEROSPACE

Aerospace Equipment Systems
Torrance

97-69288
Page 2-4
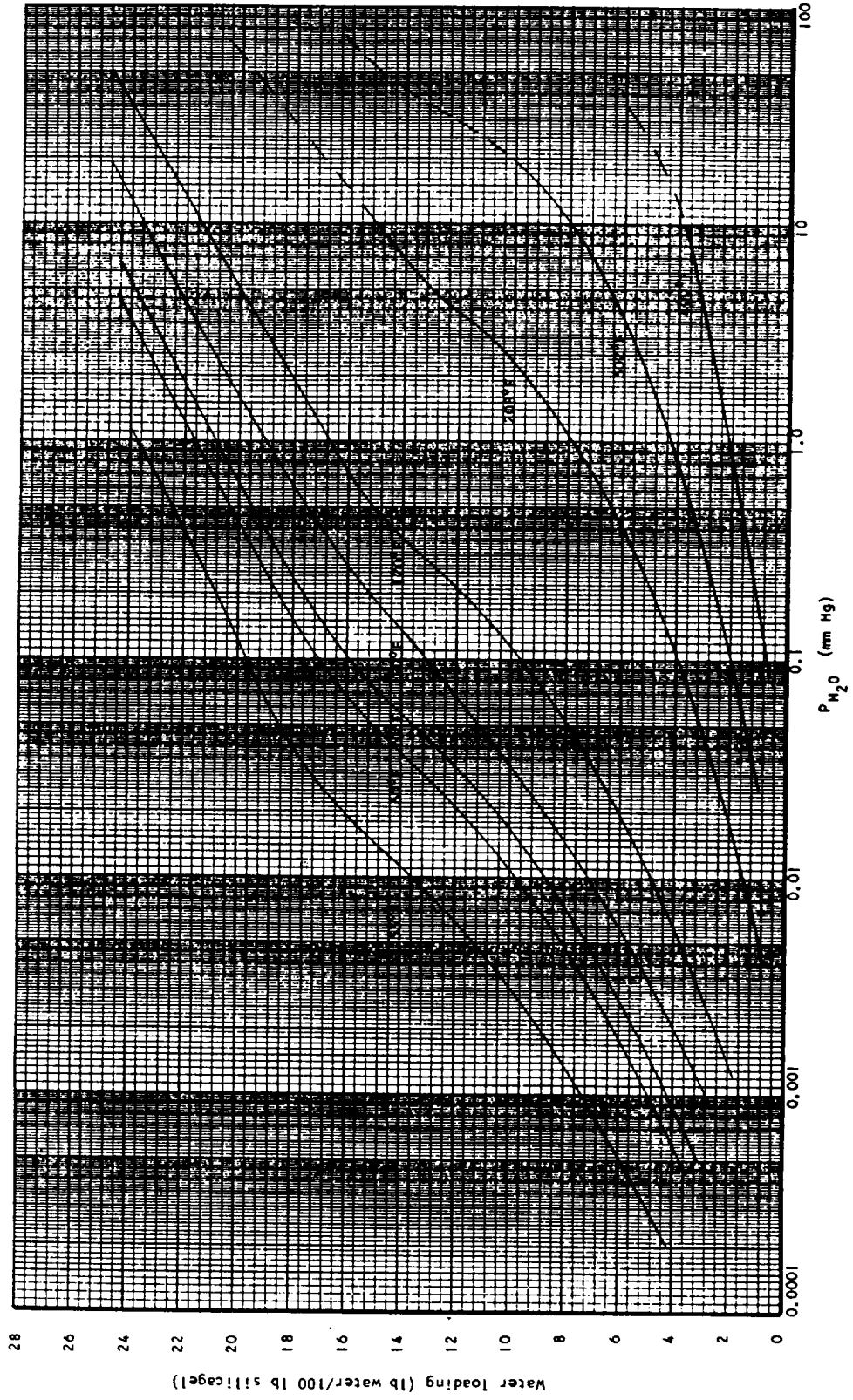
Figure 2-6. Water Vapor Equilibrium Data for Linde 13X Sorbent

AlliedSignal
AEROSPACE

Aerospace Equipment Systems
Torrance

97-69288
Page 2-5
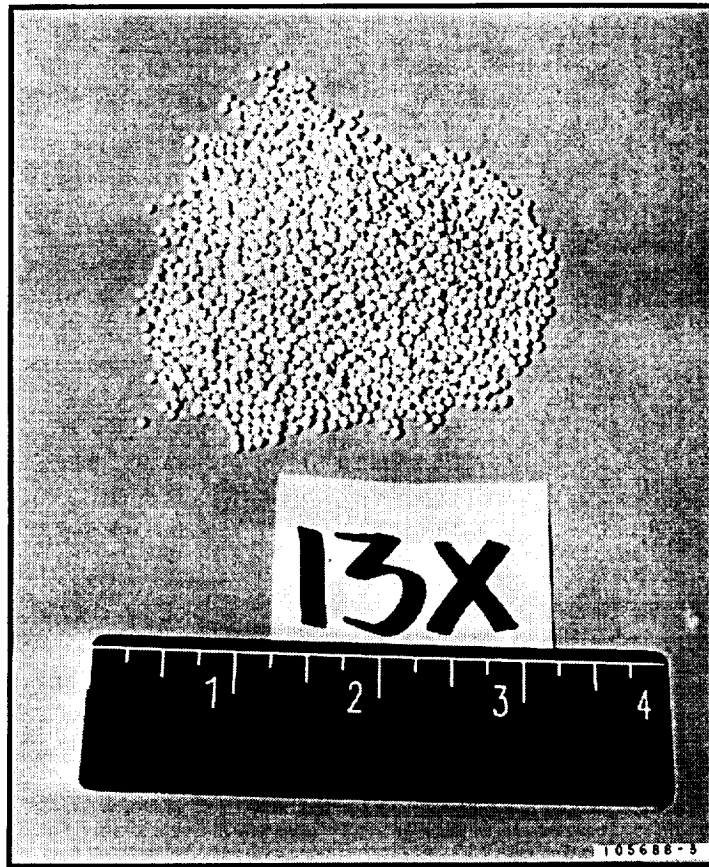
Figure 2-7. 13X Molecular Sieve

controlling the pore size and surface characteristics, the CMS will selectively adsorb CO_2 from a circulating air or oxygen stream. The CMS material also exhibits the characteristic that CO_2 adsorption is not affected by water adsorption.

The FCMS is thus effective in both moist and dry gases. The presence of moisture appears to be beneficial to the long-term stability because the CO_2 retaining complex requires the presence of a water molecule. After exposure to CO_2, the FCMS is readily regenerated by heating the material to 50° to 70°C for 30 min. There is no evidence of any release of functionalization agent during regeneration or in use. The FCMS is considered to be safe for use in a man-rated system.

Through the course of this program several different processing variants of FCMS were tested, each with slightly different characteristics and performance. These sorbents are distinguished by unique reference numbers, such as FCMS-28 or FCMS-X31.

2.2.1 Physical Form

The FCMS is formed into pellets with a length/diameter ratio = 1.0, as shown in Figure 2-8.
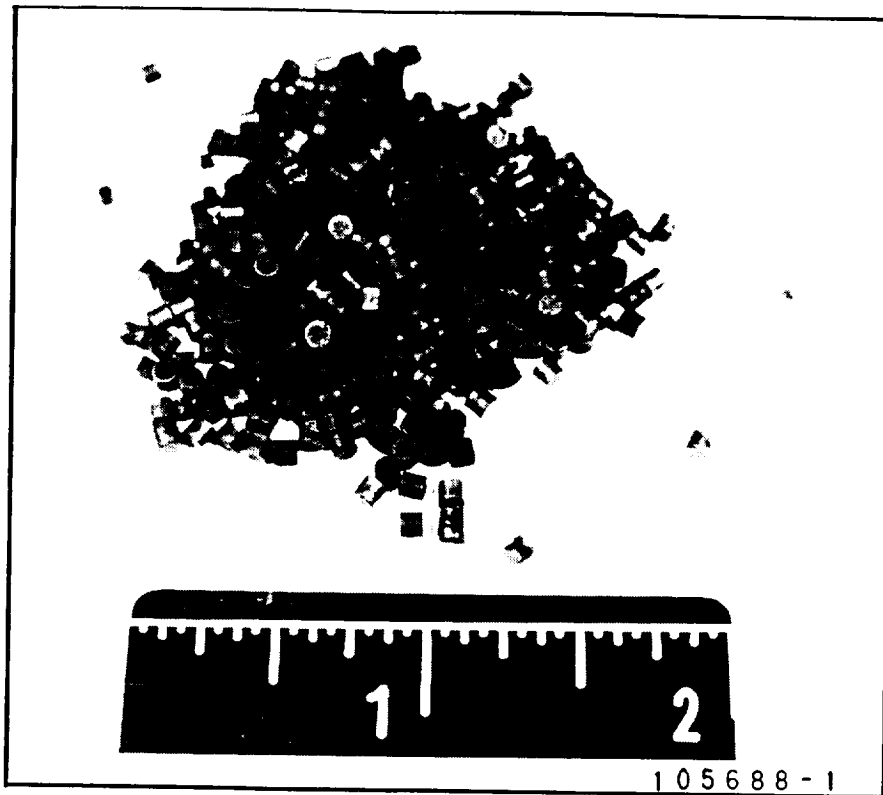
Figure 2-8. Functionalized Carbon Molecular Sieve

2.2.1.1 Material Safety; MAPTIS Testing

The FCMS material is undergoing testing for space-rated materials and the results will be logged in the material and processes technical information system (MAPTIS). The qualifications that must be met by the material include flammability, toxicity (offgassing), and thermal vacuum stability. In addition, according to NHB 8060.1C and the application of the CMS material in a human-rated flight compartment involving breathing gases in a GOX environment, the CMS material needs to meet several additional tests. These tests are as follows.

Test 1: Upward Flame Propagation—This test involves 12- by 2.5-in. sample sizes. Since the process for CMS does not preclude manufacturing at that size, this test cannot be performed. Hence, the material does not meet the requirements. Analysis and written MUA's will need to provide assurance that this material, when exposed to a standard ignition source, will self-extinguish and not transfer burning debris, which can ignite adjacent materials.

Test 2: Heat and Visible Smoke Release Rates—Once again, this test requires 4- by 4-in.-size samples. For the same reason listed above, the material does not meet this requirement. Analysis and an MUA will be written to pass this requirement.

Test 6: Odor Assessment (To Be Done Providing Passing Test 7, Sec. 4.7)—This test requires material samples with a surface area ratio of 300 cm^2 of sample

AlliedSignal
AEROSPACE

Aerospace Equipment Systems
Torrance

97-69288
Page 2-7

surface area per liter of sample container volume for testing exposed to 20.9 percent oxygen, at ambient pressure, with a 72-hr thermal exposure at 120°F. Passing is an average 2.5 rating (on a scale of 1 to 4) from five qualified odor panel members.

Test 7: Determination of Offgassing Products—This test requires a minimum of 5 g of sample material. The material is placed in an evacuated chamber and heated to 120°F for 72 hr and then cooled. Offgassing products are sampled and analyzed. Success is a total Toxic Hazard Index (T) for all volatile offgassing products of less than 0.5.

Test 13B: Mechanical Impact for Materials in Variable Pressure GOX and LOX— Success is measured if any of twenty samples does not react when struck at 72 ft-lb at the related pressure and temperature of the material application.

In addition, according to ASTM E 595-93, thermal vacuum stability requirements must be met. A screening technique is used to determine volatile control of materials when exposed to a vacuum environment. After exposed to simulated space vacuum, if the total mass loss (TML) is less than 1 percent and collected volatile condensable material (CVMC) is less than 0.1 percent, the material is accepted. To date, the material has passed flammability to an A rating according to the MAPTIS requirements. All other tests are currently underway and have not been completed.

2.2.2 Equilibrium Properties

CO_2 adsorption isotherms for the FCMS are presented on Figure 2-9 (Patent 4,810,266). The functionalized CMS has a capacity approximately twice that of the unfunctionalized material. The capacity at 25°C and 7.6 torr partial pressure is about 50 percent of that exhibited by the advanced 5A zeolite at equilibrium conditions (Figure 2-4).

2.2.3 CO_2 Adsorption in the Presence of Moisture

Dynamic tests of breakthrough capacity were conducted to establish the breakthrough characteristics of the functionalized CMS. Breakthrough tests were conducted with 1-atm dry and humid air. The results are presented in Table 2-1, and show that the CO_2 capacity was unaffected by the presence of water vapor in the inlet air stream.
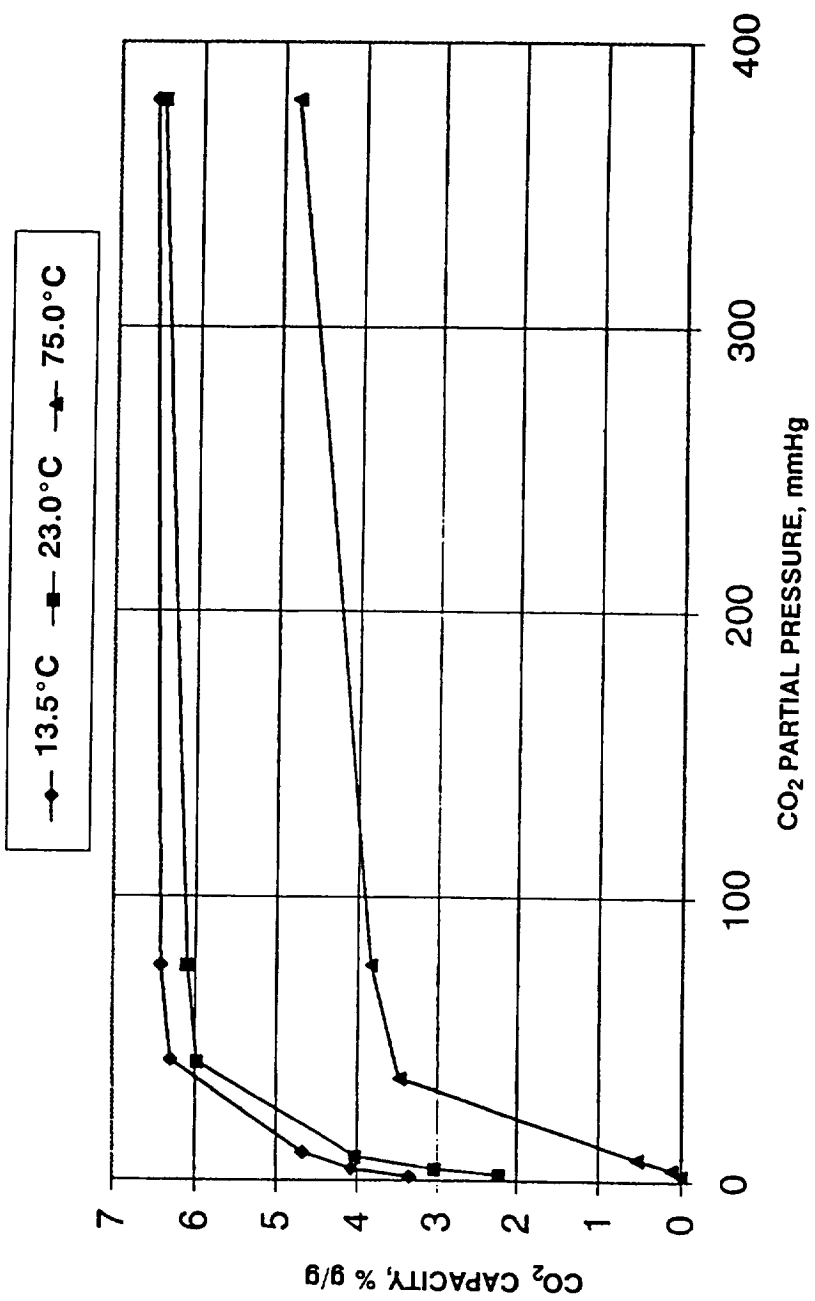
Figure 2-9. CO₂ Adsorption Isotherms for Functionalized CMS

IG-30243

TABLE 2-1
CO$_2$ BREAKTHROUGH CAPACITIES OF FCMS

Sorbent	CO$_2$, %	Relative Humidity, %	Bed Temp., °C	Capacity*, %, g/g
FCMS-X5	0.389	Dry	23 to 25	3.35
	0.389	80	24 to 28	3.38
	0.389	Dry	8.5 to 10.4	4.10
	0.389	80	9.0 to 10.5	3.84
FCMS-X5	1.008	Dry	24 to 27	4.18
	1.008	80	23 to 28	4.22
	1.008	Dry	8.4 to 11.8	4.02
	1.008	80	8.4 to 11.1	4.14
FCMS-X12	0.389	Dry	24 to 27	2.95
	0.389	80	25 to 27	2.83
	0.389	Dry	8.0 to 10.0	3.40
	0.389	80	8.0 to 10.0	3.64
FCMS-X12	1.008	Dry	24 to 27	3.39
	1.008	80	22 to 27	3.34
	1.008	Dry	13.0 to 17.0	3.51
	1.008	80	9.0 to 12.0	3.51
*At 50% Breakthrough				

Allied Signal
A E R O S P A C E
Aerospace Equipment Systems
Torrance

97-69288
Page 2-10

3. TEST PROGRAM

3.1 METHODOLOGY

A test rig was assembled to subject the experimental molecular sieve materials to the conditions experienced in a two-bed regenerable CO_2 removal system. The test setup permits the flow cycling indicated in Figure 1-1 of Section 1. The sorbent bed modules were subjected to alternating cycles of adsorbing and vacuum desorbing. All tests were conducted with air as the carrier gas and with adsorption occurring at 1.0-atm total pressure for simulated station testing, and at 3.75 psia for simulated suit testing.

3.2 TERMINOLOGY

The following terminology and definitions are used in the data analyses of the breakthrough (to saturation) and multi-cycle tests:

Breakthrough—Adsorption of CO_2 on molecular sieve beds, such as those in this program, have a typical "S" curve, where nearly all of the CO_2 is removed from the air-stream for a period of time, and then the CO_2 at the outlet will gently curve up, increasing until equal to the CO_2 at the inlet. Breakthrough is defined as the point where the CO_2 at the outlet begins to increase. Quantitatively, this could be defined as the point where more than a defined amount of CO_2 has passed through the bed. A 100 percent breakthrough curve is equivalent to a saturation curve.

Cycle—When a given bed completes a desorption half-cycle and an adsorption half-cycle.

Cycling Test—A series of equal duration adsorb and desorb half-cycles were conducted at specified conditions until the CO_2 at the outlet stabilized over multiple adsorption cycles.

Desorption—Pressure-swing regeneration of the sorbent.

50 Percent Breakthrough—Defined as the point where the CO_2 concentration at the outlet of the bed equals approximately 50 percent of the CO_2 concentration at the inlet. An 80-percent breakthrough level also was used.

Breakthrough and saturation have been defined in terms of CO_2 removal. They also can be applied to any adsorbate (i.e., water) taken up by the bed.

Half-Cycle—The period of time for a given bed to complete an adsorption or desorption cycle.

Mixed Bed—The mixed bed(s) comprise 13X and 5A zeolites. The 13X is on the air inlet side during adsorption and during desorption (reverse flow desorption). The majority of the tests were performed with approximately a 50/50 volumetric split of the two materials.

Regeneration — Removal of adsorbates from an adsorbent to restore it to a baseline state. The standard process for both sorbents is to heat the adsorbent while flowing dry nitrogen through the adsorbent.

Residence Time — The reciprocal of the number of bed volumes per second. Normally expressed in seconds.

Saturation — Saturation is the point in time when the adsorption bed no longer has capacity for CO_2. The CO_2 at the outlet will thus stabilize near the value of the CO_2 at the inlet, with slight variations due to pressure gradients and thermal effects.

Weight per Weight Capacity — The maximum mass of adsorbate adsorbed by the adsorbent. For the saturation tests, the %w/w capacity for CO_2 of a given adsorbent is identified.

3.3   TEST RIG DESCRIPTION

A schematic diagram of the thermally coupled pressure-swing test rig is presented in Figure 3-1. A photograph of the control panel and computer data acquisition system is shown in Figure 3-2.

3.3.1   Air Subsystem

In the test installation, the inlet airflow (dry) is filtered and then mixed with 100 percent concentrated carbon dioxide gas to obtain the specified CO_2 partial pressure. The airflow can then be bubbled through a tank of deionized water to humidify the air to the desired level. Any free moisture resulting from humidification is removed in a water trap.

The airflow is bypassed around the adsorption beds while the airflow rate and the water and CO_2 concentrations are adjusted. When the flow conditions have stabilized, the bypass is closed and the rig is switched to computer control. Two-way solenoid valves are energized as required to direct the airflow to one of the beds and to switch the other bed to the laboratory vacuum source. The outlet flow from the adsorbing bed is discharged to the laboratory ambient. This mode is continued for the specified half-cycle time and then the valve positions are switched to open the inlet side of the bed filled with sorbate to the vacuum source and to expose the desorbed bed to the airflow.

During desorption, the test rig is nominally configured to apply vacuum to what was previously the inlet face of the bed during the adsorption cycle.

3.3.2   Desorption Subsystem

For the desorption portion of the cycle, the bed is switched to the laboratory vacuum system, which is shown in Figure 3-3. The test rig is located very close to the vacuum tank. Two 600-cfm roots-type blowers produce a vacuum of approximately 10 microns at the rated flow. The vacuum tank (approximately 12-cu ft volume) located
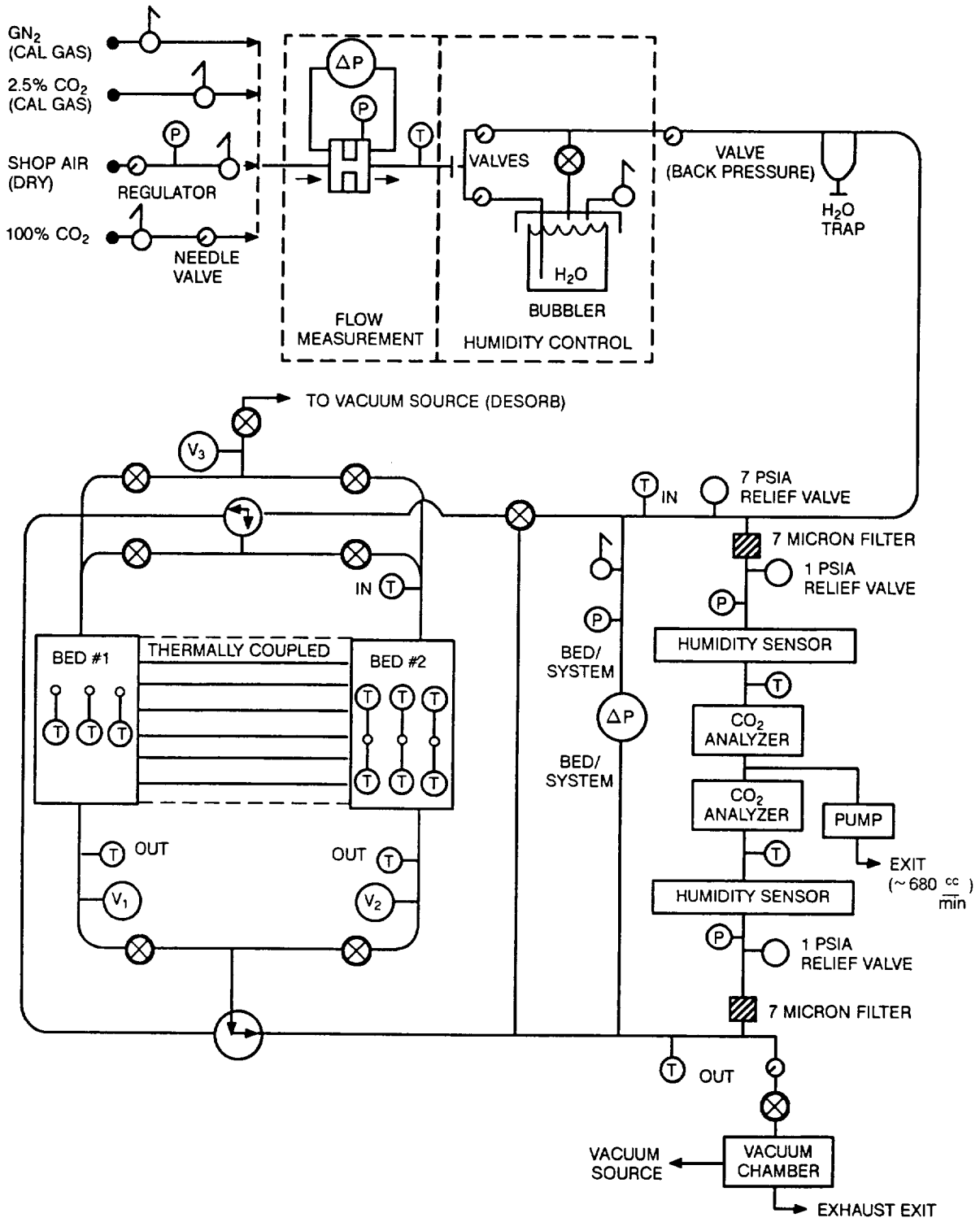
Figure 3-1. Thermally Coupled Pressure-Swing Adsorption Test Rig

IG-32006A

AlliedSignal
A E R O S P A C E

Aerospace Equipment Systems
Torrance

97-69288
Page 3-3

105688-5
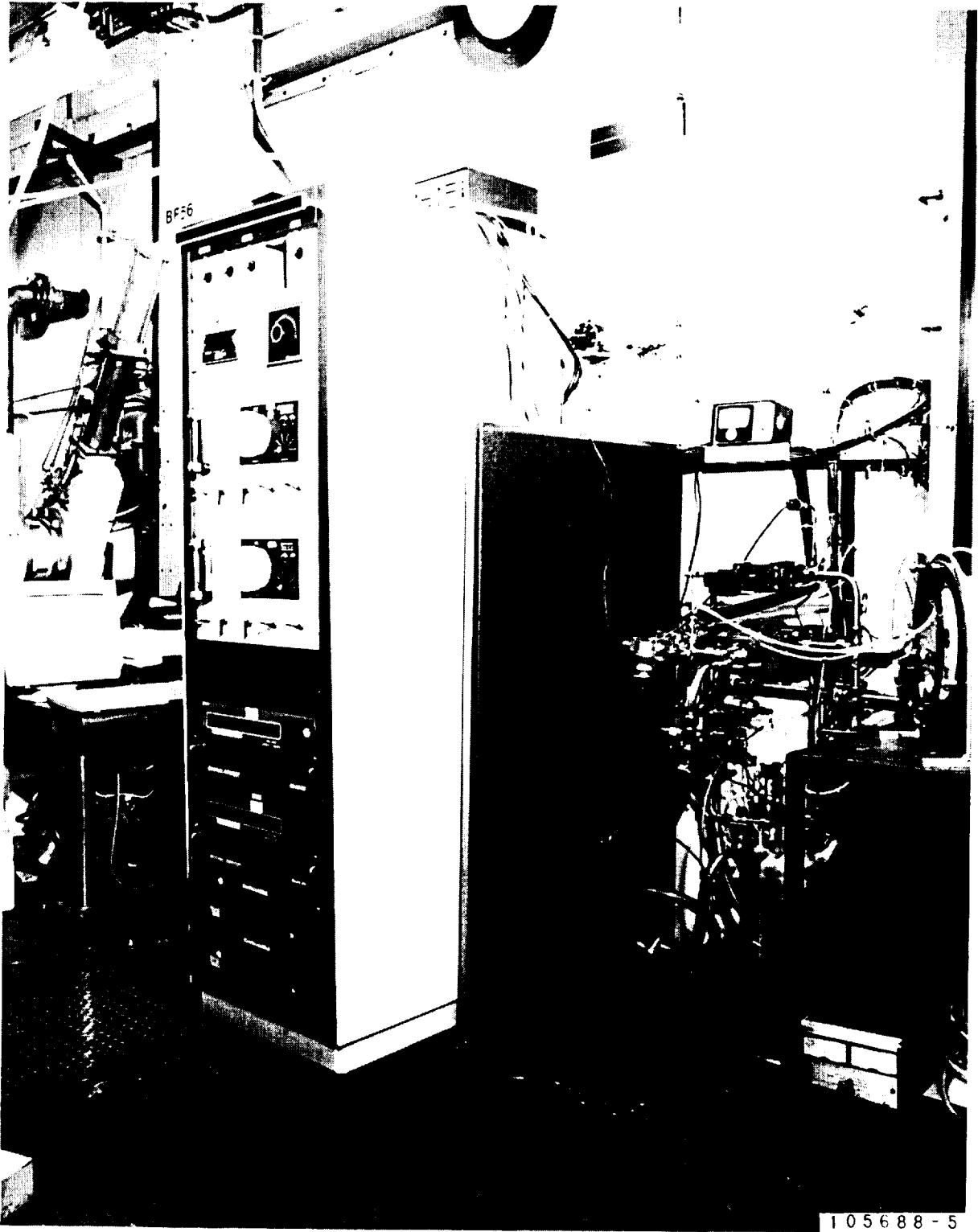
Figure 3-2. Test Rig, Control Panel, and PC

F-68796

AlliedSignal
AEROSPACE

Aerospace Equipment Systems
Torrance

97-69288
Page 3-4
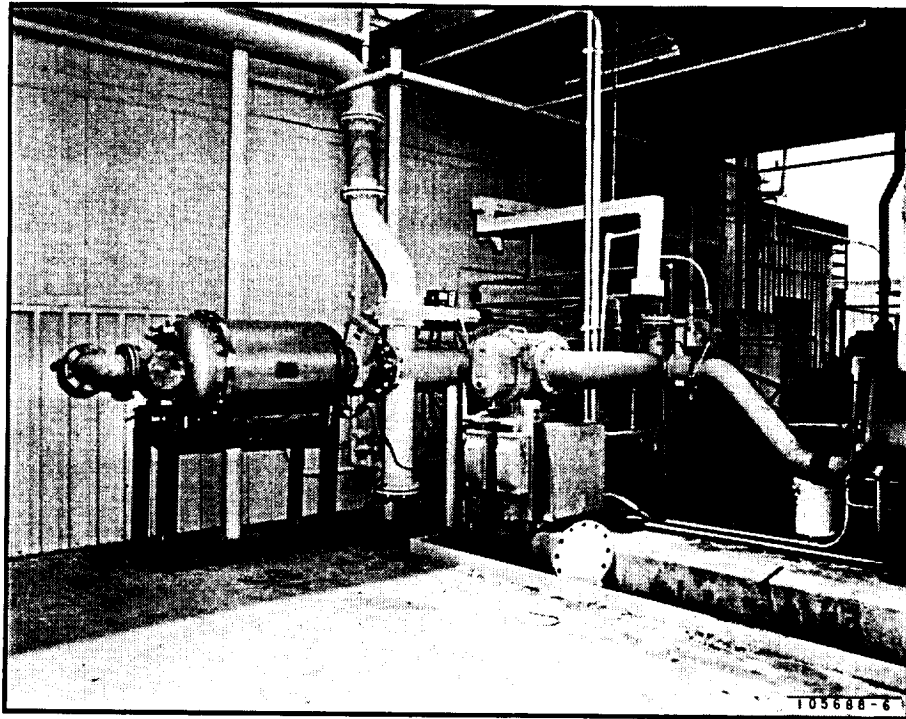
Figure 3-3. Laboratory Vacuum System

upstream of the blowers and after the test beds is a liquid-nitrogen-cooled cold trap. During this test series, the cold trap was operated to freeze out any water vapor flow before the vacuum pumps.

3.3.3 Control Program

A control sequencing program automatically cycles the valves, alternating adsorption and desorption cycles between the two beds. The length of the half-cycle time can be set to any chosen duration.

3.3.4 Instrumentation

Gas sampling ports are located such that flow conditions at the inlet and outlet of the adsorbing bed are monitored. A small compressor is used to draw gases from the downstream side of the test bed into the analyzer. It takes approximately 1 min for the sample gas to reach the analyzers. The CO_2 analyzer responds nearly immediately while the humidity analyzer stabilizes after 1 to 4 min.

Instrumentation is indicated in Figure 3-1 and the sensor characteristics are summarized in Table 3-1.

3.3.4.1 Dewpoint Analyzer

Dewpoint of the inlet and outlet airflow stream was determined using a General Eastern Hygro-M4 humidity analyzer equipped with a Model SIM-12H two-stage heated

sensor downstream and a non-heated 111H sensor upstream. The instrument uses optical condensation hygrometry to measure the water vapor content in the air stream.

Optical condensation hygrometry works on the chilled-mirror principle. A metallic mirror is cooled until it reaches a temperature at which condensation begins to form on it. The dew layer is detected and the mirror is held at that temperature. The mirror temperature, measured with a platinum resistance thermometer, is an accurate indicator of the dewpoint. The overall accuracy of the system is $\pm 0.2°C$. The sensor is rated over a range of -15° to +25°C upstream and -10° to 85°C downstream. The sample flows through the meter at 0.25 to 2.5 l/min.

3.3.4.2 CO$_2$ Analyzer

A Beckman Model 868 Non-Dispersive Infrared Analyzer was used to measure the CO_2 concentration in the inlet and outlet air streams. Analysis was based on a differential measurement of adsorption of infrared energy. Within the analyzer, two equal energy infrared beams are directed through two parallel optical cells, a flow-through sample cell, and a sealed reference cell. The differential infrared energy adsorbed in the cells is a measure of the CO_2 concentration in the sample.

The instrument was calibrated for a maximum CO_2 concentration of 2.5 percent. The Beckman specification states: (1) zero drift ± 1 percent/24 hr full-scale, (2) repeatability and noise ± 1 percent of full scale (2.5 percent CO_2), and (3) sensitivity = 200 ppm of CO_2. Sample flow was set at 500 to 1000 cc/min (1 to 2 scfh). The instrument was calibrated once each day using dry nitrogen and 2.5 percent CO_2 calibration gas.

3.3.5 Data Acquisition

Data acquisition and control of the pressure-swing apparatus is accomplished by an IBM PC/AT compatible computer. All data are processed by two Metrabyte DAS-8-PGA 16-channel, analog-to-digital converter boards (A-D board) installed in the PC. All loop signals (up to 16 thermocouples, and up to 16 pressure transducers or voltage signals) are connected to the A-D board via two 16-channel multiplexers. Outputs for control of the sequencing solenoid valves are controlled by a digital output board (installed in the PC) connected to a nine-channel mechanical relay board.

The data acquisition system scans data every 0.5 sec and records the data at a user-defined interval. The test rig can be configured for one- or two-bed operation.

During test operation, selected temperature, pressure, and gas composition readings were displayed on the computer monitor.

3.3.6 Bed Design

Three different bed configurations were investigated: adiabatic, thermally coupled, and isothermal.

TABLE 3-1

SENSOR/INSTRUMENTATION

Channel	Description	Manufacturer	Serial #	Range	Accuracy
1-0	Bed 4, 2/L thermocouple	AlliedSignal	NA	0 to 500°F	±2°F
1-1	Outlet 1/H thermocouple	AlliedSignal	272081323	0 to 500°F	±2°F
1-2	Bed 5, 2/M thermocouple	AlliedSignal	NA	0 to 500°F	±2°F
1-3	Inlet 2/I thermocouple	AlliedSignal	272081324	0 to 500°F	±2°F
1-4	Upstream analysis temp.	AlliedSignal	272081455	0 to 500°F	±2°F
1-5	Bed 6/B thermocouple	AlliedSignal	272082889	0 to 500°F	±2°F
1-6	Bed 4/A thermocouple	AlliedSignal	272082893	0 to 500°F	±2°F
1-7	Downstream analysis temp.	AlliedSignal	272081452	0 to 500°F	±2°F
1-8	Bed 5/C thermocouple	AlliedSignal	272082890	0 to 500°F	±2°F
1-9	Bed 1/D thermocouple	AlliedSignal	272082891	0 to 500°F	±2°F
1-10	Inlet1/G thermocouple	AlliedSignal	272081311	0 to 500°F	±2°F
1-11	Bed 3/F thermocouple	AlliedSignal	272082895	0 to 500°F	±2°F
1-12	Bed 2/E thermocouple	AlliedSignal	272082892	0 to 500°F	±2°F
1-13	Outlet 2/J thermocouple	AlliedSignal	272081312	0 to 500°F	±2°F
1-14	Voloflow Temp	AlliedSignal	272081214	0 to 500°F	±2°F
1-15	Bed 6, 2/N thermocouple	AlliedSignal	NA	0 to 500°F	±2°F
2-1	Upstream analysis press.	MKS Baraton	22958	0 to 1000 torr	0.1 %
2-2	Bed pressure, P1	Viatran # 2186AD3T68F0	16264481	0 to 20 psia	0.1 %
2-3	Downstream analysis press.	MKS Baraton	26756	0 to 1000 torr	0.1 %
2-4	Orifice pressure	IMO	279013149	0 to 100 psia	0.1 %
2-5	Diff. bed pressure, dP2	Sensotec	279012742	0 to 2.5 psid	0.1 %
2-6	Diff. orifice pressure	Viatran	279013086	0 to 50 in H_2O	0.1 %
2-7	Diff. orifice pressure	Sensotec	279013268	0 to 0.5 psid	0.1 %
2-8	Dewpoint analysis, in	General Eastern, Hygro-H4	235010460	-80 to +80°C	± 0.02%
NA	Dewpoint sensor	General Eastern, 111H	235010462	-15 to +25°C	± 0.02°C
NA	Flow meter	Fisher and Porter	44D618	0 to 100% max flow	± 5 %
2-9	CO_2 analysis, in	Beckman Industrial, Model 868	209010545	0 to 100% full scale	8% total* (max)
2-10	Dewpoint analysis, out	General Eastern, Hygro-H4	235010483	-80 to +80°C	± 0.02%
NA	Dewpoint sensor	General Eastern, SIM-12	209010671	-10 to +85°C	± 0.02°C
NA	Flow meter	Fisher and Porter	44D619	0 to 100% max flow	± 5 %
2-11	CO_2 analysis, out	Beckman Industrial, Model 868	209010571	0 to 100% full scale	12% total* (max)
NA	Absolute pressure gage	Wallace & Tiernam	231200409	0 to 75 psi	±0.1%
NA	Differential pressure gage	Barton Instruments	231080036	0 to 40 in. H_2O	±0.1 %
NA	Vacuum gage	Hasting # VT-5B	3707	0 to 100 microns	±0.5 %
2-13	Vacuum gage/ chl 1	MKS	231181009	0 to 450 microns	± 10 microns*
2-14	Vacuum gage/ chl 2	MKS	231181009	0 to 450 microns	± 10 microns*
2-15	Vacuum gage/ chl 1	MKS	220012870	0 to 450 microns	± 10 microns*
*Based on calibration curves					

3.3.6.1 Adiabatic

The adiabatic bed is a cylindrical shaped stainless steel canister with a 1-in. manifold at the inlet and exit. The cylinder has a 0.0875-in. wall thickness with a vacuum flange at the top of the canister. Up to six thermocouple ports are provided to monitor the material temperature in the sorbent at different depths, as well as to measure the air temperature in and out of the manifolds. Screens located at the bottom and top hold the material in place, and springs are placed above the top screen to keep the material packed. A photograph of the adiabatic bed is shown in Figure 3-4a.

3.3.6.2 Thermally Coupled

The thermally coupled test bed consists of a heat exchanger core accompanied by screens, springs, manifolds to secure the material in place and direct the air flow approximately. The core has 63 channels and a face area approximately 0.3 by 0.5 in. and a flow length of 3.3 in. Photographs of the beds are provided in Figure 3-4b. Attached to each of the four core faces is a manifold with 1-in. ducts. Each manifold supports a series of eight springs attached to screens that secure the adsorbent material within the tubes of the core. An O-ring type seal is used between the core and manifold.

3.3.6.3 Isothermal

The thermally coupled bed can be run isothermally by removing the sorbent from one of the two beds and flowing constant-temperature water through this side. The water temperature and flow rate are adjustable. This water loop is used only for heating/cooling the desorbing/adsorbing bed and is independent of the air loop.

3.3.7 Operations

Airflow with the specified moisture and CO_2 concentrations was set with the flow bypassing around the test beds. Data acquisition was initiated by the computer program to monitor the rig operations and to initiate the valve sequencing operations. Testing began when the rig was switched from the bypass mode and airflow was directed to the test bed for the initial adsorption half-cycle.

Prior to pressure-swing testing, the beds were pretreated to obtain a sorbate concentration < <1.0 percent. The pretreatment was done by placing a test bed in an oven at an appropriate regeneration temperature for the material (400°F for 13X and 5A material; 120°F for FCMS) with a flow of dry nitrogen through the adsorbent bed for at least 6 hr. In later tests for FCMS, pressure-swing regeneration replaced the heat regeneration.

3.4 TEST MATRIX

Performance tests of the sorbent with different operating regimes were performed on the different sorbents under both station and suit conditions. The tests performed are detailed in the Appendix. First-year testing was primarily performed on zeolites 5A and 13X in an adiabatic test bed at open-loop station conditions (1 atm).
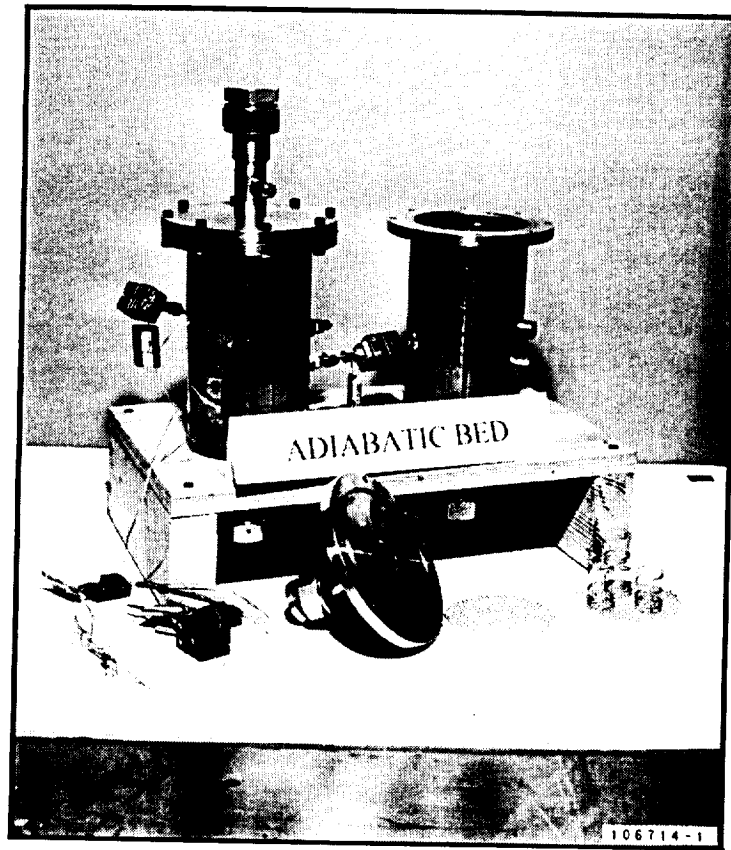
a. Adiabatic Bed
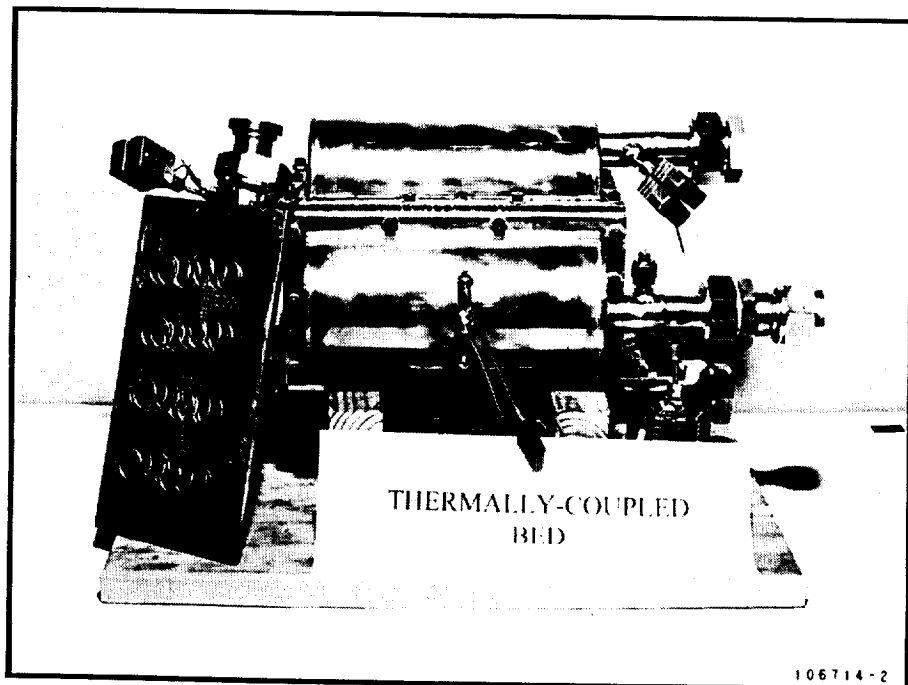
b. Thermally Coupled/Isothermal Bed

Figure 3-4. Test Beds

AlliedSignal
A E R O S P A C E

Aerospace Equipment Systems
Torrance

97-69288
Page 3-9

Second-year testing was much more extensive and included different materials and operating conditions. Zeolite testing replaced the 5A with an improved 5A sorbent similar to the Space Station material, and several functionalized carbon molecular sieve materials were investigated. Initial tests were performed with X24, but the X28 material shows substantially better performance and the majority of the FCMS results in this report focus on this latter material.

The zeolite 5A-50 and FCMS X28 materials were subjected to a series of standard tests at both station and suit conditions, as well as additional tests, including performance in different types of sorbent beds (adiabatic, isothermal, and thermally coupled) with different operational protocol.

3.5 TEST DATA INTERPRETATION

3.5.1 Breakthrough Testing Interpretation

Breakthrough data on a regenerated bed at representative conditions were obtained to identify an appropriate cycle time, as well as to indicate the efficiency of the bed via the capacity of the material. This dynamic capacity is a function of many variables, including flow distribution, pressure drop, thermal effects, and regeneration effectiveness.

3.5.2 Multi-Cycle Pressure-Swing Interpretation

Multi-cycle pressure swings show dynamic performance of the material utilizing vacuum desorption. The data are a continuous monitoring of the two beds, 1 and 2 (alternating). When examining the graphs of cyclic data, it should be noted that:

- The graphs plot the data for both beds. The data for each are analyzed separately.

- There is a lag time in the sensor readings after a cycle change. For the CO_2 analyzer, this lag is as long as 4 min.

- The CO_2 adsorption rate (lb CO_2/hr) is based on the CO_2 adsorption rate of the last cycle of any given test.

- Under the defined test conditions, it appears that the CO_2 removal by the adsorption bed decreases for a short time before stabilizing.

- For isothermal tests, Bed 1 has water flow; thus, only Bed 2 data should be considered.

The tests ended when a performance trend was established, or when saturation was achieved (based on the type of test selected). Airflow was placed in a bypass mode. The bed(s) could be removed for regeneration before retesting and/or new beds installed for continued testing. Once in the bypass mode, the rig could be shut down and data recording discontinued.

4. BED DESIGN INVESTIGATION

A series of investigations was performed to confirm that the test bed design and test method were accurate and effective. Some aspects of the bed design investigated were:

- Pressure-swing regeneration effectiveness

- Packing density

- Pressure drop

- Flow distribution

4.1 PRESSURE-SWING REGENERATION EFFECTIVENESS

The effectiveness of the pumpdown was investigated to assure repeatable and consistent results compared with heat and nitrogen regeneration. Saturation tests and pressures during desorption were used as a basis of comparison to determine if vacuum desorb was as effective as heat and nitrogen regeneration.

4.1.1 CMS

Saturation test with the CMS materials demonstrated that the breakthrough characteristics of the sorbent following vacuum desorption to 100 microns shows similar performance as that following a standard heat and nitrogen regeneration (Figure 4-1).

Different vacuum desorption durations, ranging from 1 min to 2 hr, were tested to characterize the performance as a function of regeneration time.

A series of tests was run to isolate variables and determine which affect the pumpdown most significantly. Some such variables include bed loading of H_2O and CO_2, temperature, pump capacity, rig and bed capacitance, kinetics of the material, bed shape, and flow length. The effects of some of these variables are shown in Figure 4-2.

A bed loaded with various loadings was tested. The loading conditions were as follows:

- Six-minute half-cycle, 3.1 percent CO_2 and H_2O loading

- Six-minute half-cycle, 5 percent CO_2 (high CO_2) and H_2O loading

- Six-minute half-cycle, 3.1 percent CO_2 loading (CO_2 only)

- Regenerated bed (no loading)

- 100 percent CO_2 and H_2O saturation

A completely regenerated bed took less than 2.5 min to simply evacuate all the air (no loading of CO_2 or H_2O). A dry bed (no presence of water) had the best pumpdown rate.
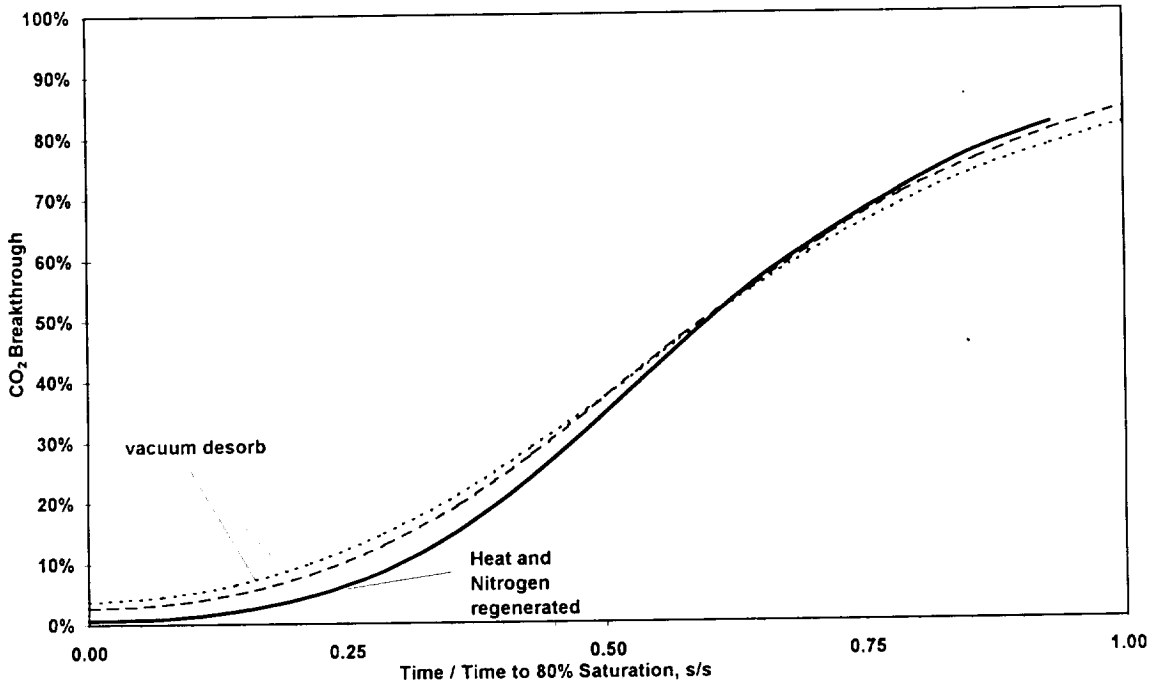
Figure 4-1. Heat and Nitrogen Regeneration Compared with Vacuum Desorption
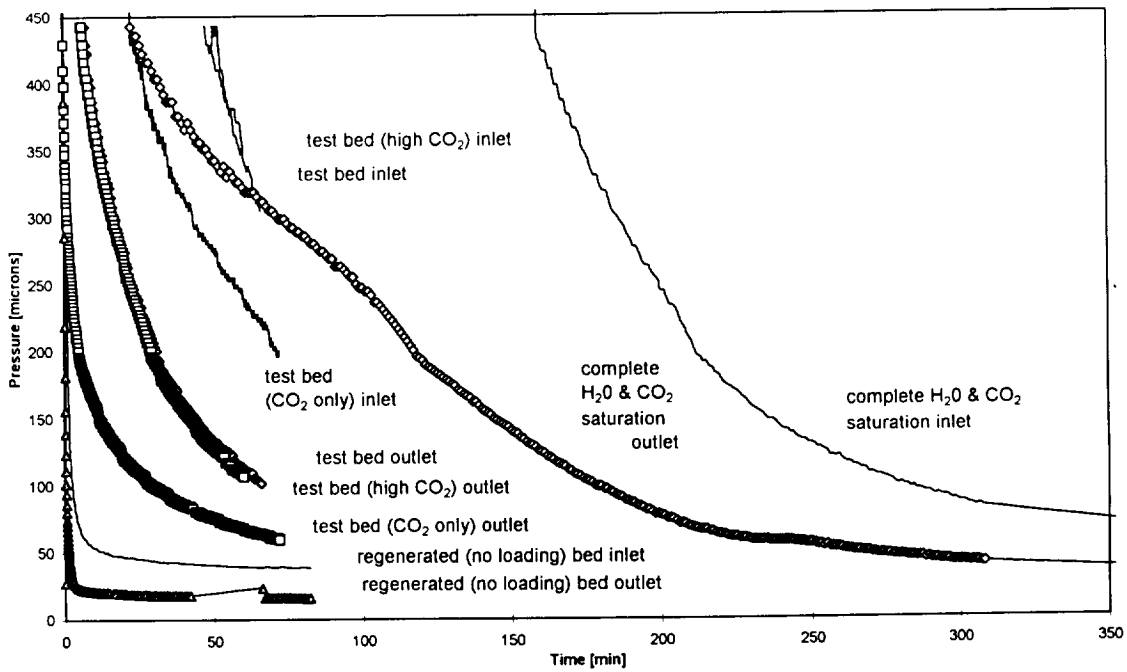

Figure 4-2. Desorb Pressures Versus Time for Various Loadings

Various bed shapes were tested (Figure 4-3). The bed with a shorter flow length showed a faster pumpdown, particularly on the side of the bed far from the pump.

The adiabatic bed pumped down faster than a thermally coupled bed (Figure 4-4), but not significantly so. This suggests that choking in the flow passages and manifold were not a driving force. In addition, the capacitance of the rig was nearly negligible, since the pumpdown of the thermally coupled bed positioned very close to the vacuum pump and further downstream in the test rig were nearly identical.

4.1.2 Zeolite

In a two-bed zeolite pumpdown, zeolites respond differently to vacuum compared to the CMS (see previous figures); the rate of pumpdown to the inlet and the outlet of the bed crossed one another (Figure 4-5).

This suggests that as water vapor was released in the closest portion of the bed to the vacuum (13x), the CO_2 in the furthest part of the bed (5A-50) was being readsorbed onto the 13x. This did not, however, seem to affect the desorption effectiveness, as evidenced by the good results in the cyclic testing (Figure 4-6).

The saturation results, however, were not as expected after long-duration desorbs; allowed to desorb as long as overnight, the bed performance did not improve compared with that for a short half-cycle time (Figure 4-7).

4.2 PACKING DENSITY

Each sorbent and bed configuration has a unique packing density. This variation impacts the pressure drop of the system and the mass of sorbent that can be packed into a given bed volume. Tests were conducted to obtain experimental data on the packing density for pellets of different size and shape and in different bed configurations. These data were incorporated into analytical models of pressure drop, performance, and heat transfer.

Essentially, the packing densities were used in conjunction with the pellet densities to give the voidage fraction of the bed, the voidage fraction being the ratio of the difference between the pellet and packing densities and the pellet density. This number is significant because it is a contributing factor to pressure drop, as well as to the performance of the removal system. A tradeoff exists between minimizing pressure drop while maximizing the quantity of sorbent material and removal performance for a given volume.

There were two basic tests run on all of the sorbent materials: (1) the graduated cylinder test and (2) the three-channel test. Different sorbents tested included zeolites 13X and 5A-50 and FCMS-X21, X24, and X28, as well as a placebo material that was nonreactive. The materials were heat regenerated prior to test to ensure more accurate results by stripping away the increased mass of the sorbent material after prolonged exposure to air.
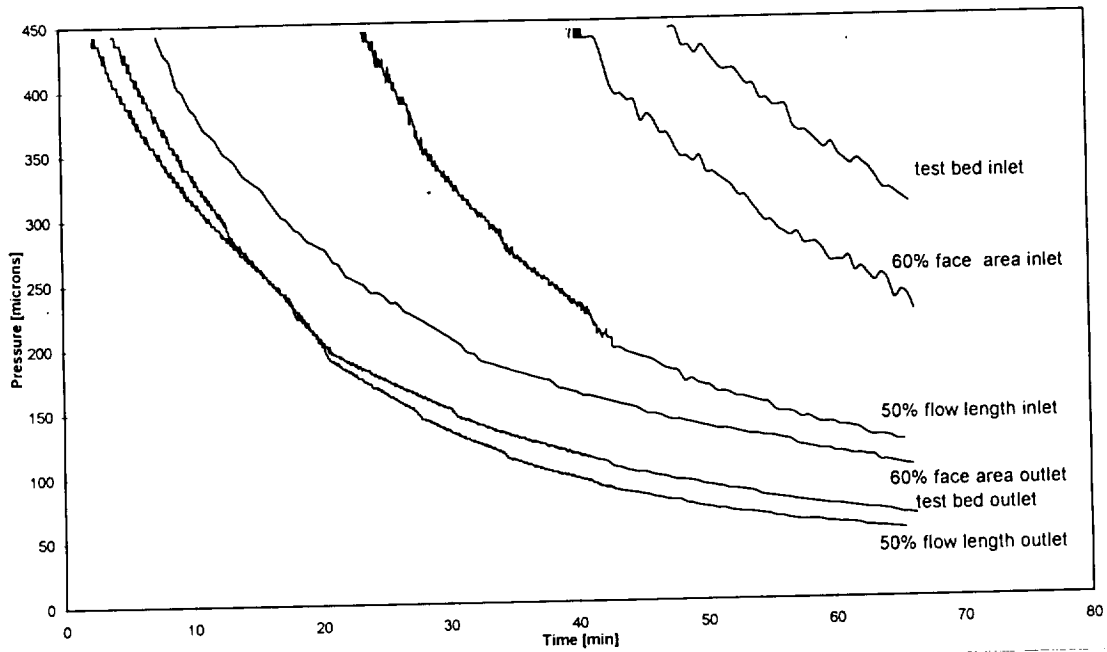
Figure 4-3. Desorb Pressure Versus Time for Various Shaped Beds
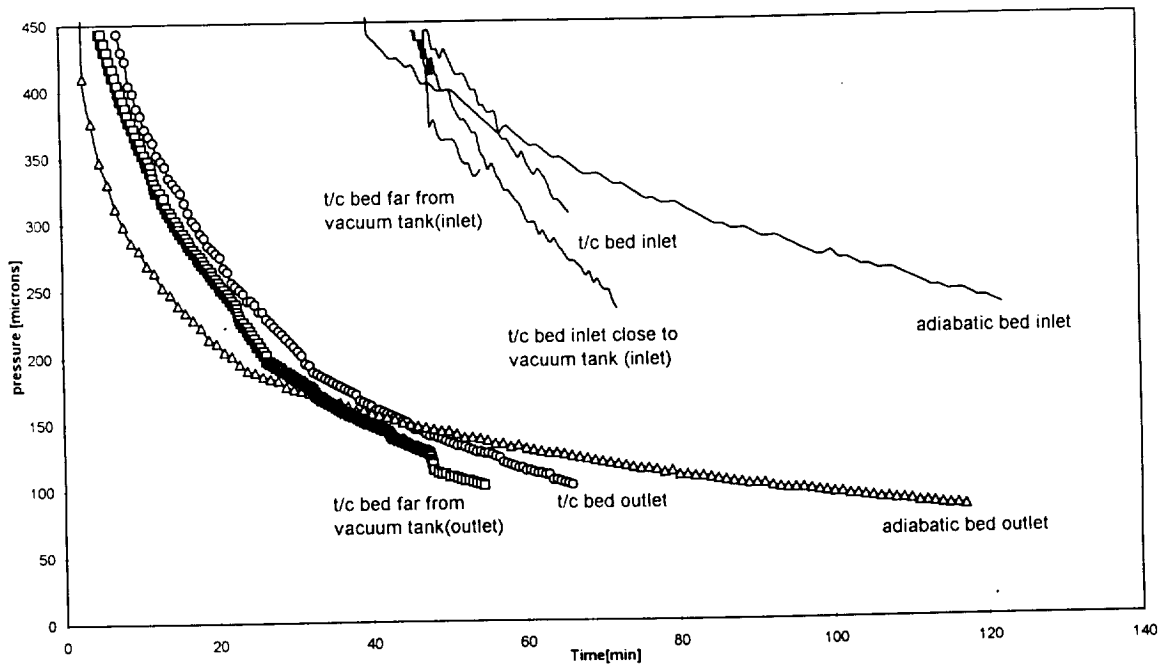
Figure 4-4. Thermally Coupled Versus Adiabatic Pumpdown
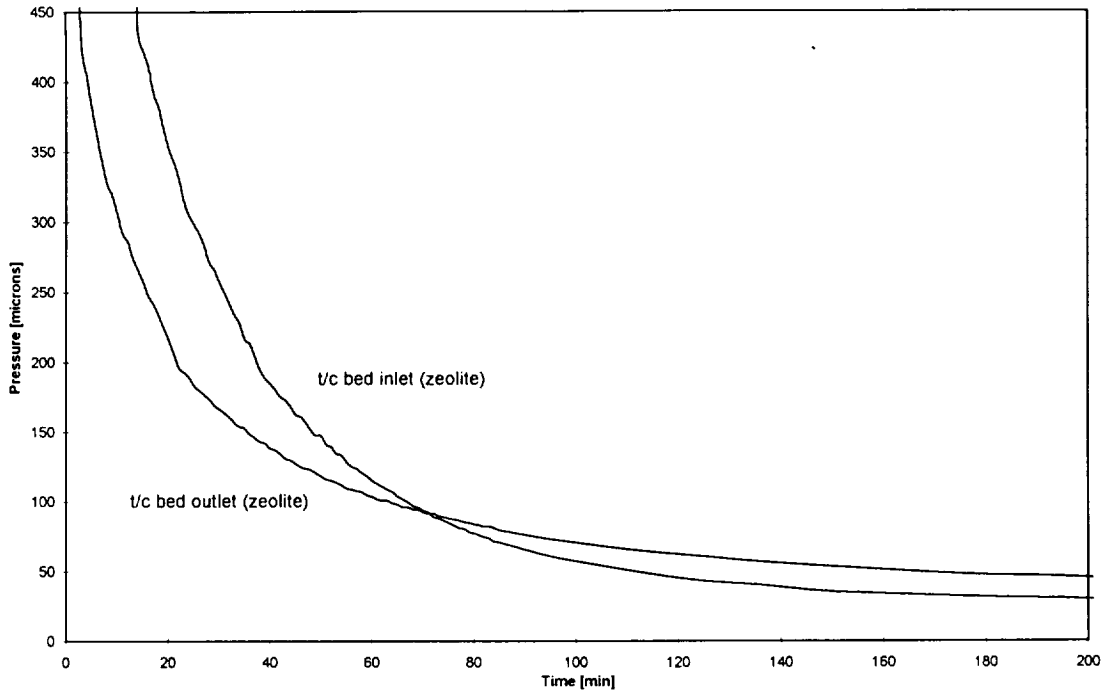
Figure 4-5. Zeolite Pumpdown Crossing (Crossover)
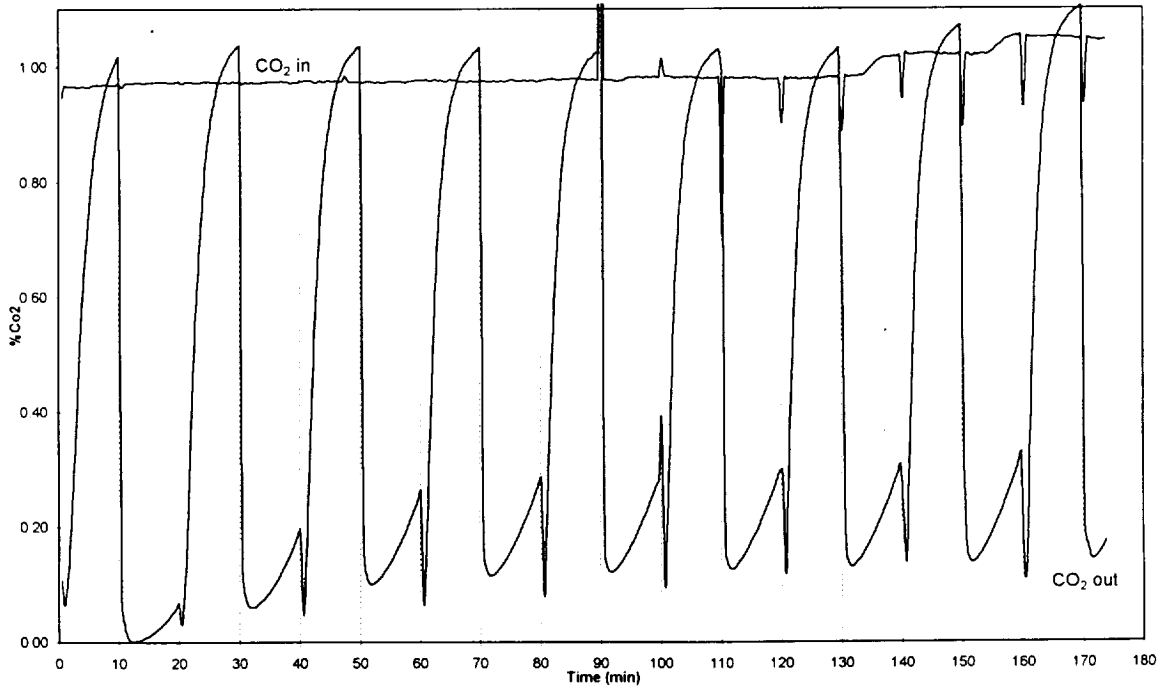
Figure 4-6. Zeolite Cyclic Performance Data

AlliedSignal
AEROSPACE
Aerospace Equipment Systems
Torrance

97-69288
Page 4-5
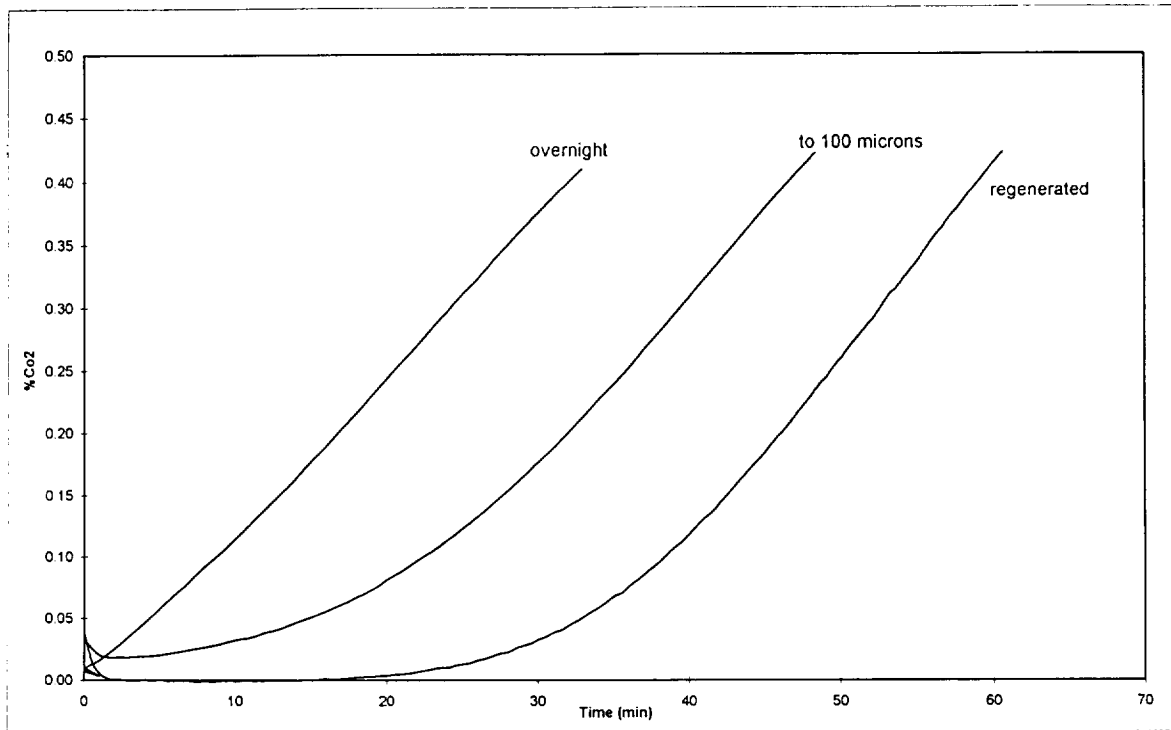
Figure 4-7. Adsorption Following Different Duration Desorb Half-Cycles

For large volume sizes (compared to the pellet size), the smaller the pellet size, the more material can be packed in a given area. In the three channel tests, a block with three 0.33 by 0.49 channels was packed with sorbent material. The purpose of this test was to investigate the wall effects on packing density. The literature indicates that the void fraction (directly related to the packing density) for particle dimensions close to channel dimensions can be expressed as the number of particle diameters as a dampened sinusoidal function of distance from a wall. Figure 4-8 (Fraas, A. and Ozisik, N.) illustrates the strong effect of particle size on the packing density when the particle size is close to the channel dimension, as in a thermally coupled bed. Lab testing found the 0.01-in. pellets gave the best void fraction, followed by the 0.06-in. and 0.08-in. pellets, respectively. This demonstrated that it is difficult to link particle size to packing density.

In addition, the results were affected by packing techniques. Differing packing techniques, such as effects of tapping, shaking, and loading (placing external weights to force the materials closer) affected the total packing density. Tapping the sides of the vessel with a rubber mallet, shaking the vessel on a vibrating surface during filling, and placing a load on top of the pellets between the pouring stages were factors shown to have a positive effect on the packing density. The results of the packing density tests are summarized in Table 4-1.

AlliedSignal
AEROSPACE
Aerospace Equipment Systems
Torrance

97-69288
Page 4-6
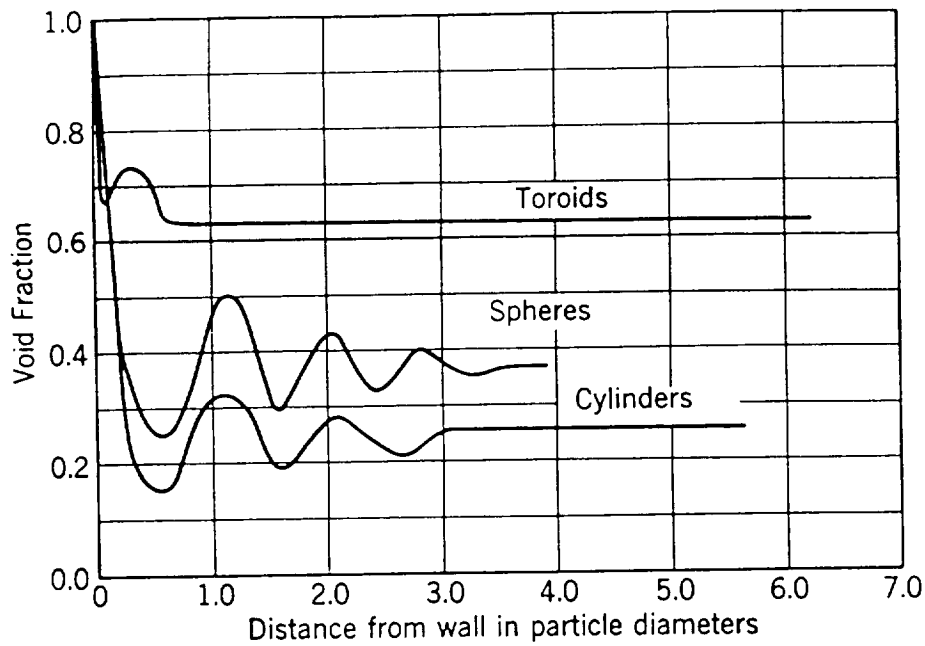
Figure 4-8. Local void Fraction Versus Distance

TABLE 4-1

PACKING DENSITY

Material	Pellet Dimensions, Dia [in.] by Length [in.] (cylindrical)	Vessel	$\rho_{material}$, g/cc	$\rho_{packing}$, g/cc	Void Fraction, ϵ
FCMS-X21	0.1 by 0.1	Three channel	1.190	0.702	0.410
	0.1 by 0.1	Graduated cylinder	1.190	0.766	0.357
	Pellets crushed	Three channel	1.190	0.865	0.273
	0.1 by 0.1	Beaker	1.190	0.748	0.372
FCMS-X24	0.08 by 0.08	Three channel	1.209	0.597	0.506
	0.08 by 0.08	Graduated cylinder	1.209	0.577	0.523
FCMS-X21	0.10 by 0.10	Graduated cylinder	1.190	0.888	0.253
Zeolite 5A (Grace)	0.0768 (cylindrical)	Graduated cylinder	1.702	0.756	0.555
Zeolite 13X (Grace)	0.0768 (spherical)	Graduated cylinder	1.872	0.721	0.615
5A-50	0.084 (spherical)	Graduated cylinder	2.230	0.735	0.669
FCMS-X28	0.08 by 0.08	Three channel	1.332	0.606	0.545
	0.08 by 0.08	Graduated cylinder	1.332	0.600	0.550
	0.08 by 0.08	Graduated cylinder	1.332	0.621	0.534
Placebo	0.06 by 0.06	Three channel	0.874	0.537	0.386

AlliedSignal
AEROSPACE

Aerospace Equipment Systems
Torrance

97-69288
Page 4-7

The FCMS and zeolites thus have similar packing and material densities. When evaluating CO_2 removal system this has several implications:

- The zeolites have a higher capacity for CO_2 than FCMS, but, in the presence of humidity, require a desiccant of approximately the same volume as the sorbent, in line prior to the CO_2 sorbent bed. The CO_2 capacity per unit volume of sorbent is thus 40 percent higher with FCMS than with the combined zeolites.

- As the voidage fractions are similar, the FCMS system will also have a lower pressure drop, thus also reducing the blower power required.

4.3 PRESSURE DROP

Pressure drop across the adsorbent bed is an important design parameter and typically controls the bed size. The pressure drop for three materials was measured to obtain reliable data for the current size and shape of the adsorbents using a proven test technique. The materials tested were Grace 5A (cylindrical) Grace 13X (spherical), and CMS-X21 (cylindrical).

4.3.1 Pressure Drop Test Rig

An existing test rig, shown in Figure 4-9, was used for test. The test fixture is a glass column with a bore of 1.88 in. and an overall length of 12 in. Airflow enters at the column base and is discharged to the laboratory ambient. The first section of the column is filled with glass spheres to a depth of 3.0 in. to promote uniform distribution. A perforated steel plate with a fine mesh screen is used to support the molecular sieve pellets. The pellets were poured into the column and then the assembly was vibrated to settle, and finally, the length of the pellet bed was adjusted to 3.0 in.

A calibrated orifice was used to measure airflow. The orifice inlet pressure was measured using a precision gauge. Pressure drop was measured using a slant-tube water manometer.

4.3.2 Pressure Drop Test Results

Pressure drop across the graduated cylinder with only glass beads and perforated plate is obtained first. The delta-P for the glass beads is considered as the tare and is subtracted from the overall delta-P to obtain the pressure drop across the 3.0-in. stack of FCMS pellets. The final pressure drop, corrected for density and expressed as delta-P per inch of bed length, is presented in Figure 4-10. The same procedure was followed for the 5A and 13X materials, as illustrated in Figures 4-11 and 4-12, respectively. A comparison of the pressure drop across the three different materials is presented in Figure 4-13.

4.4 FLOW DISTRIBUTION

The flow distribution of the heat exchanger bed was investigated to ensure even flow distribution. This information was obtained with the use of a hot wire anemometer.
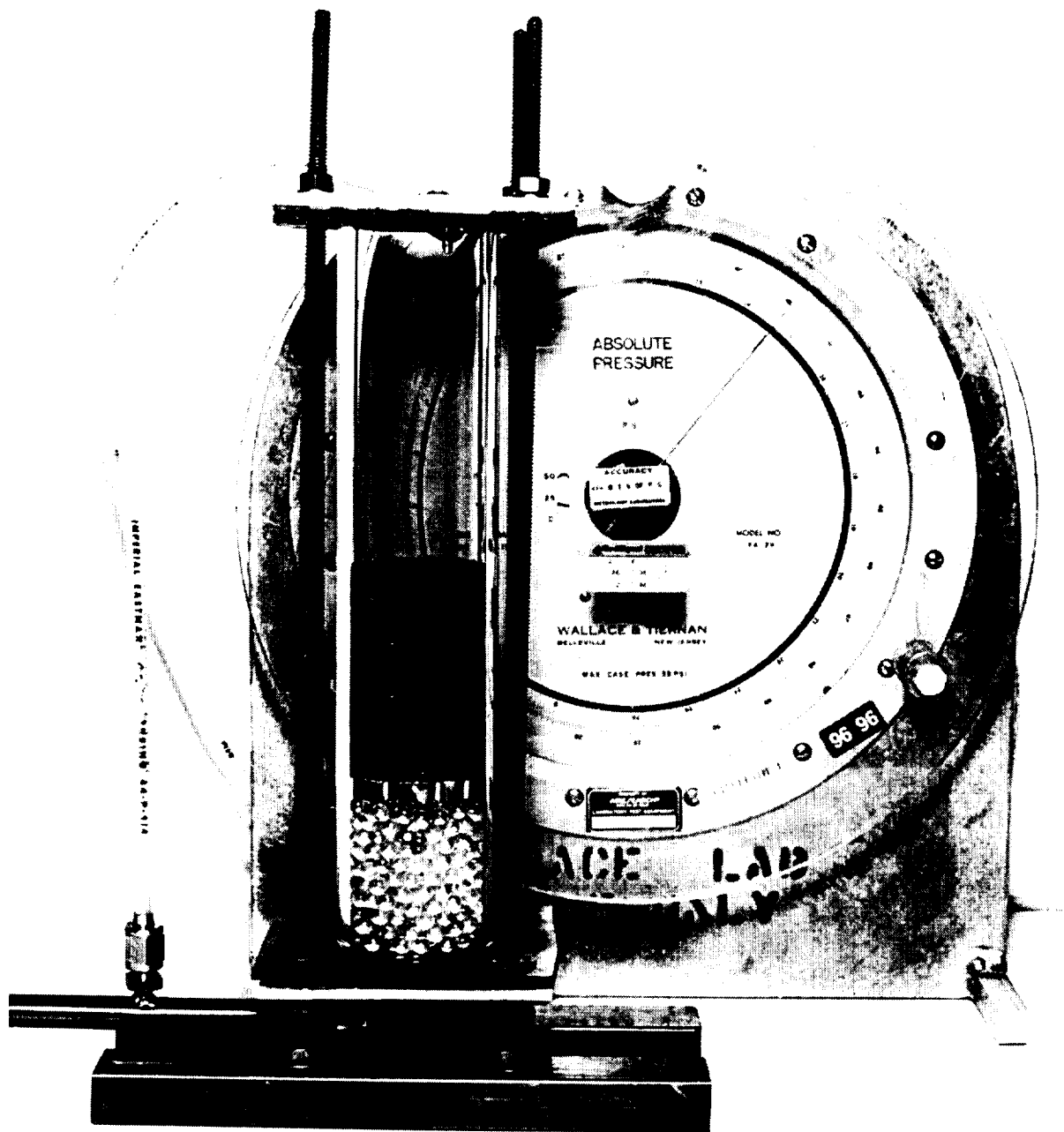
105851-1

Figure 4-9. Glass Tube Test Rig

AlliedSignal
AEROSPACE

Aerospace Equipment Systems
Torrance

97-69288
Page 4-9

CMS CORRECTED PRESSURE DROP

$y = 11.694x^{1.3580}$

Corrected Pressure Drop, Sigma Delta-P, in. H2O/in. Bed Length

Airflow, Lb/min
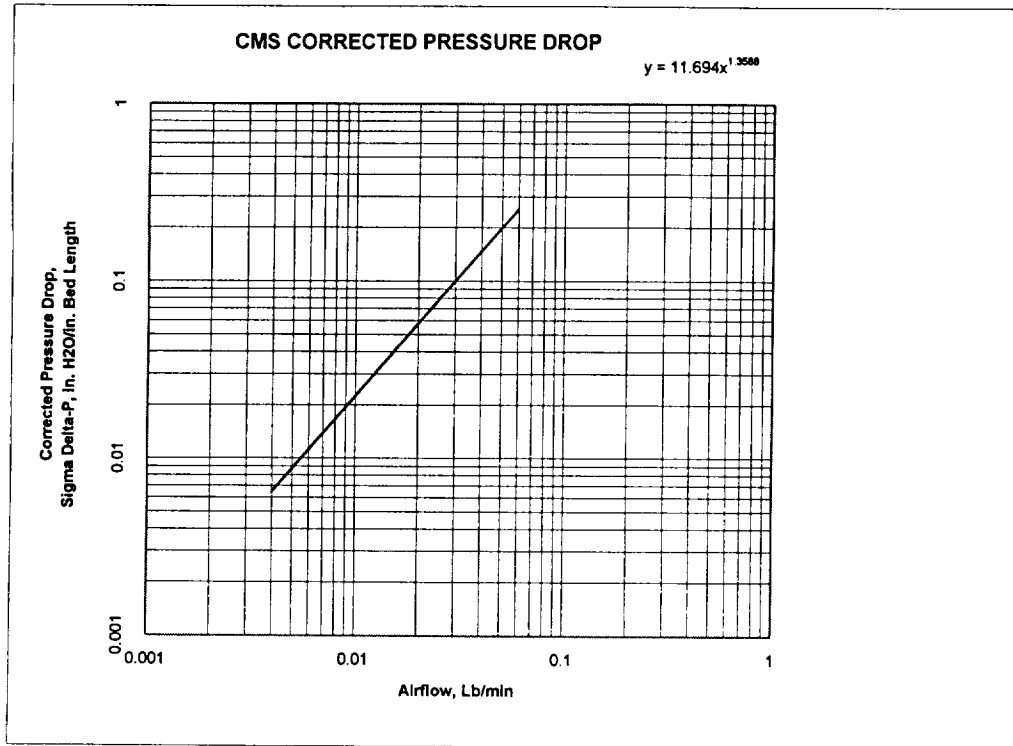
Figure 4-10. CMS (0.01 by 0.01 Cylindrical) Corrected Pressure Drop

5A BED CORRECTED PRESSURE DROP

$y = 19.303x^{1.4586}$

Corrected Pressure Drop, Sigma0 Delta-P, in. H2O per in. Bed Length

Air Flow, lb/min
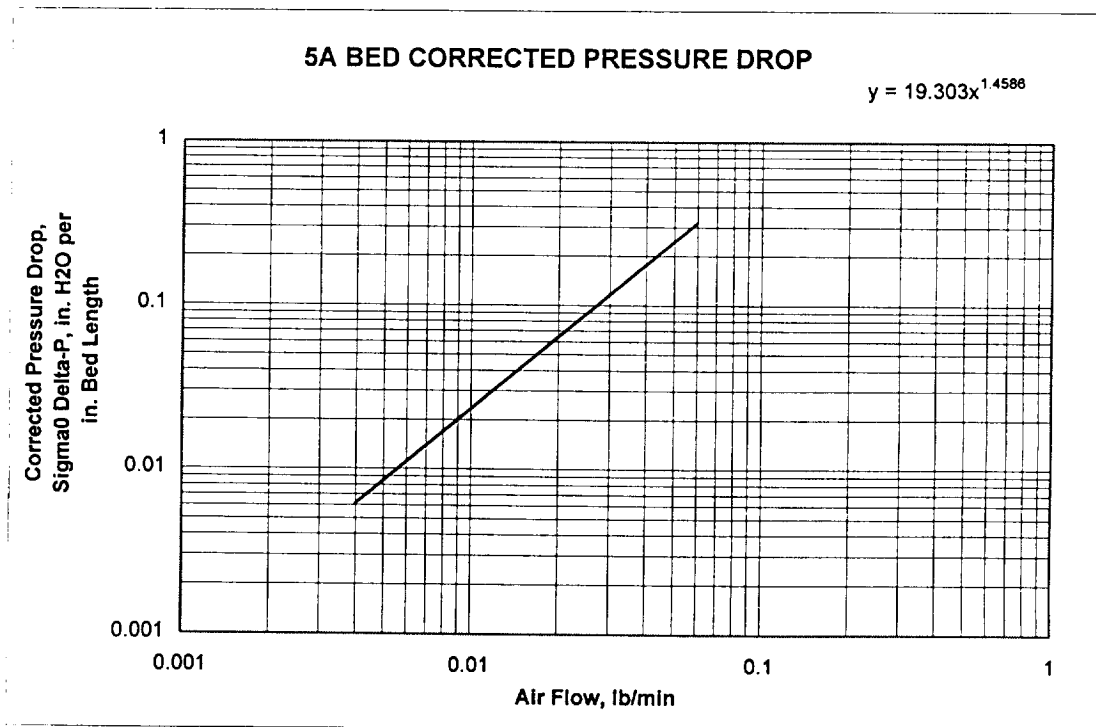
Figure 4-11.   Pressure Drop Across Grace 5A (Cylindrical) Bed

13X BED CORRECTED PRESSURE DROP

$y = 17.168x^{1.4754}$
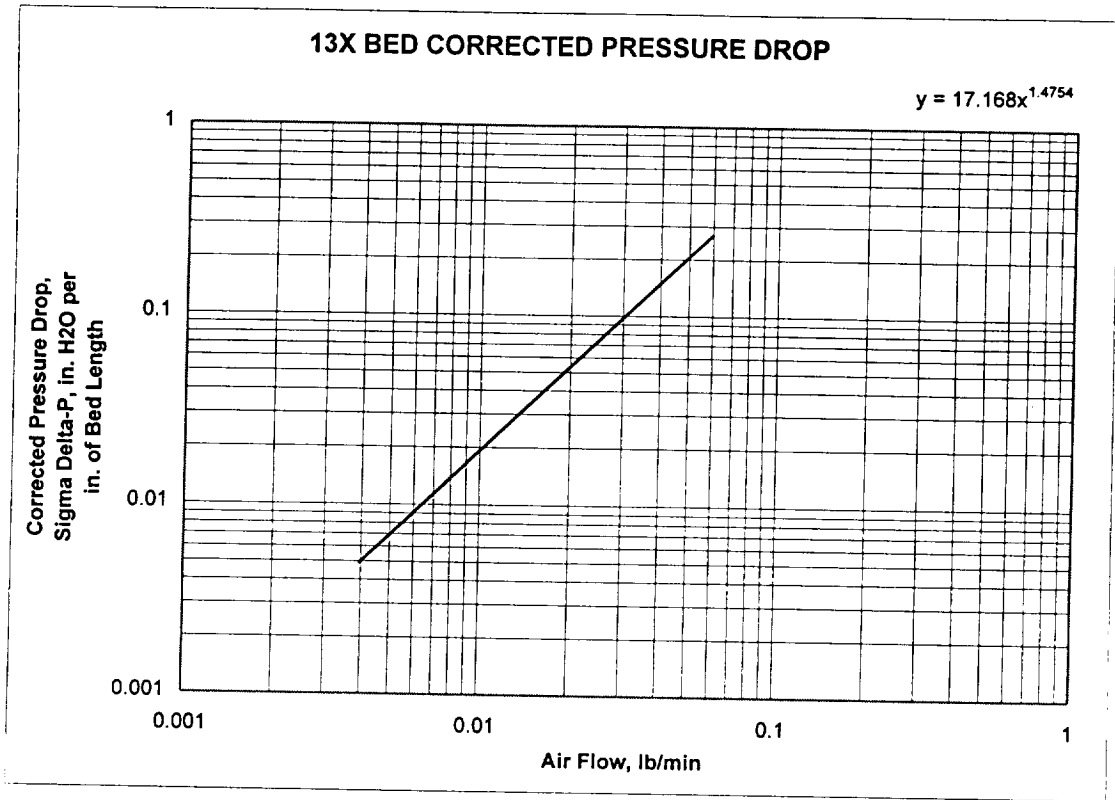
Figure 4-12. Pressure Drop Across Grace 13X (Spherical) Bed
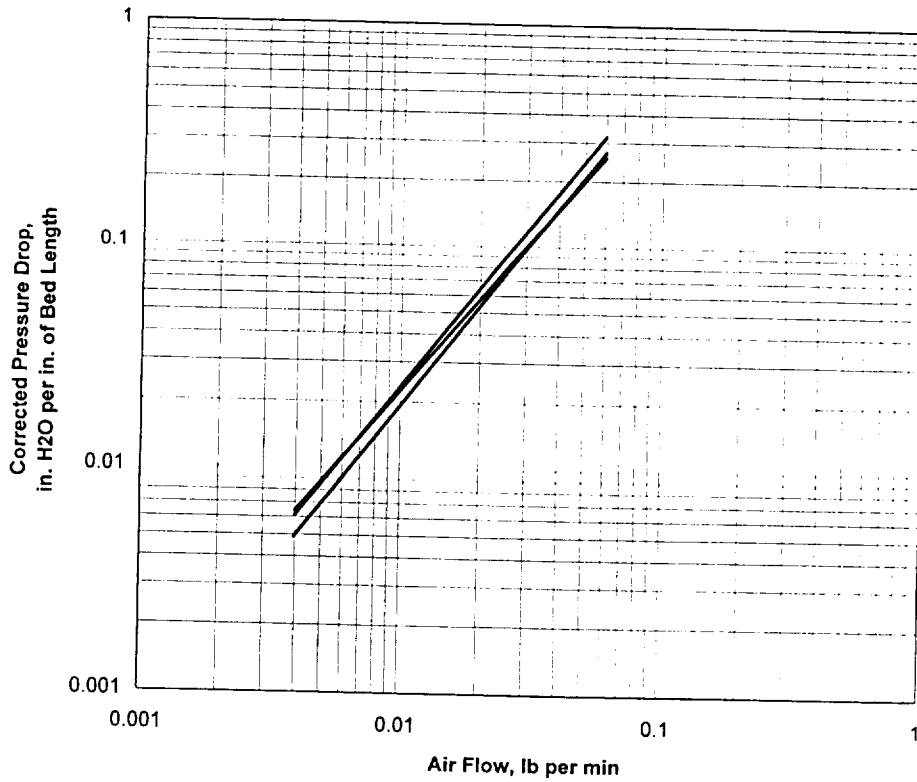
Figure 4-13. Comparison of Pressure Drop for Three Different Materials

AlliedSignal
AEROSPACE
Aerospace Equipment Systems
Torrance

One of the manifolds was removed and the air velocity coming out of each port was measured and recorded (Figure 4-14). The data were then tabulated and plotted on a three-dimensional surface graph (Figure 4-15). The rows are numbered from S1 to S7, with S1 being closest to the inlet side, and the channels were numbered 1 though 9. The graph indicates that the flow rate was greatest at the inlet (S1) and ramped down as S6 was approached. Spikes occurred in the vicinity of S7; however, this was expected due to the U-shaped flow, resulting in an increase in pressure due to stagnation of flow. The results of this test indicate that, excluding packing inconsistencies, the flow distribution is as expected and relatively uniform.
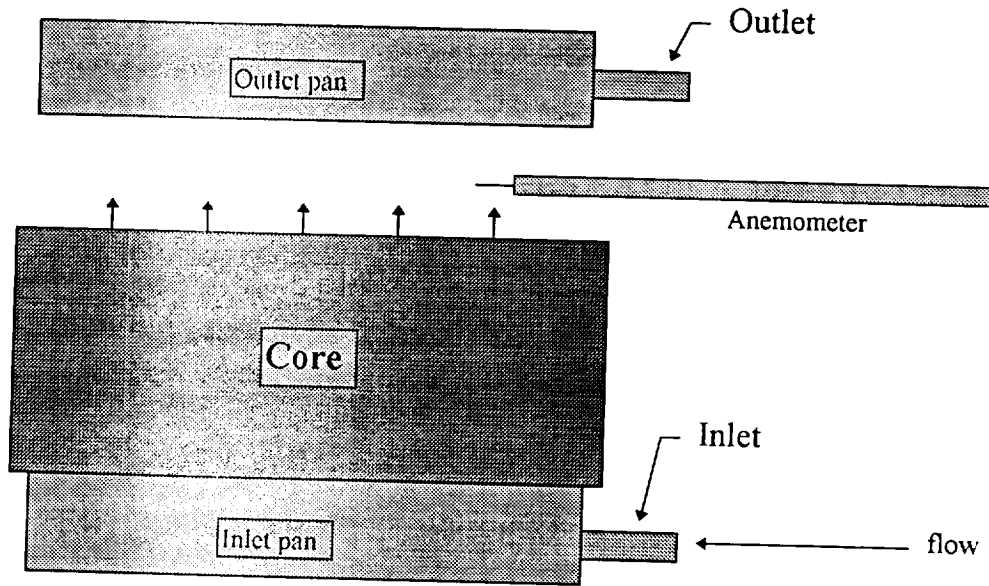
Figure 4-14. Flow Distribution Test Setup
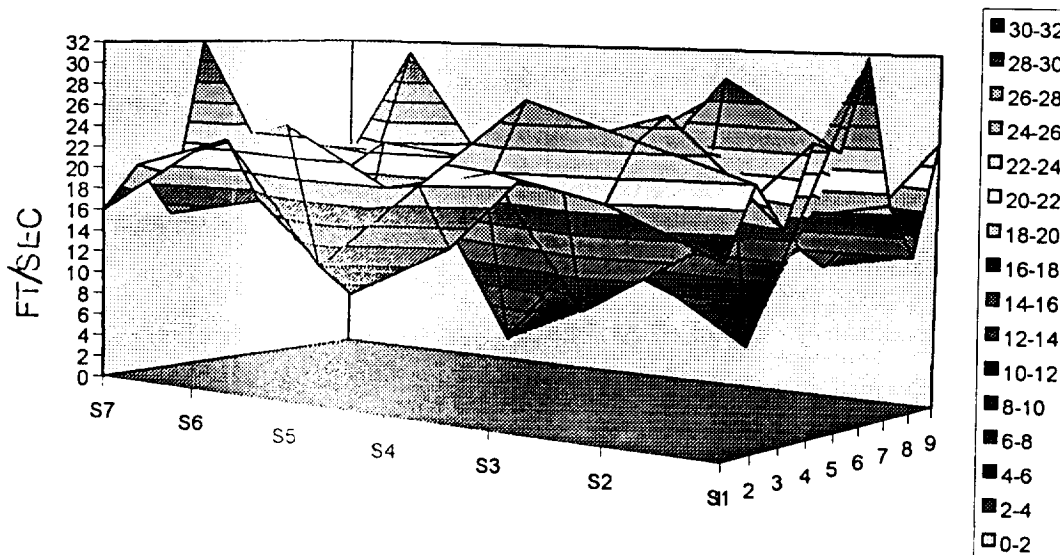
Figure 4-15. Flow Distribution Test Results

5. TEST RESULTS

Testing of the two sorbents was performed following the protocol presented in Section 2. Baseline breakthrough and cyclic data were obtained for both the FCMS and the zeolites at the suit and station conditions defined in Table 1-1. Further investigation of the sorbents was performed. Presented here are results of three key specialty topic areas potentially affecting the sorbent performance—thermal effects of bed design, bed aspect ratio, and air save in which the two beds are pressure equalized at valve switchover

5.1 BREAKTHROUGH CURVES

Table 5-1 highlights the breakthrough performance. The breakthrough curves for both CMS and zeolite yielded nearly identical results for test at suit conditions (Figure 5-1), but showed wider differences under station conditions (Figure 5-2).

TABLE 5-1 BREAKTHROUGH SUMMARY DATA	Suit		Station	
	FCMS	Zeolite	FCMS	Zeolite
Time to breakthrough, min	10	11	43	60
CO_2 removal efficiency, percent	48	31	79	80
CO_2 capacity, w/w	3.25	3.56	2.19	2.38
Water removal efficiency, percent	65	83	92	95
Water capacity, %w/w	2.45	1.52	4.84	5.07

These results show the difference in performance between suit and station conditions and the effects pressure, CO_2 concentration, residence time, and flow rate have on the system. These data also give preliminary performance data for system design.

5.2 BASELINE CYCLIC DATA

Table 5-2 shows cyclic performance for FCMS and zeolite (in a thermally coupled bed) at suit and station conditions. Figures 5-3 and 5-4 graph the performance of two pairs of beds. The results of the best bed, although similar to the opposing bed, are shown in the table.

Cyclic data provided a variety of information concerning the removal of CO_2 and H_2O. In all cases the first half-cycle showed the best performance (after the bed was regenerated); this should represent the best possible performance as the bed is completely regenerated. The cyclic curves level off to a repeatable steady-state performance after a few cycles (less than ten cycles, typically) with a lower performance, indicating less than 100 percent regeneration during desorb.
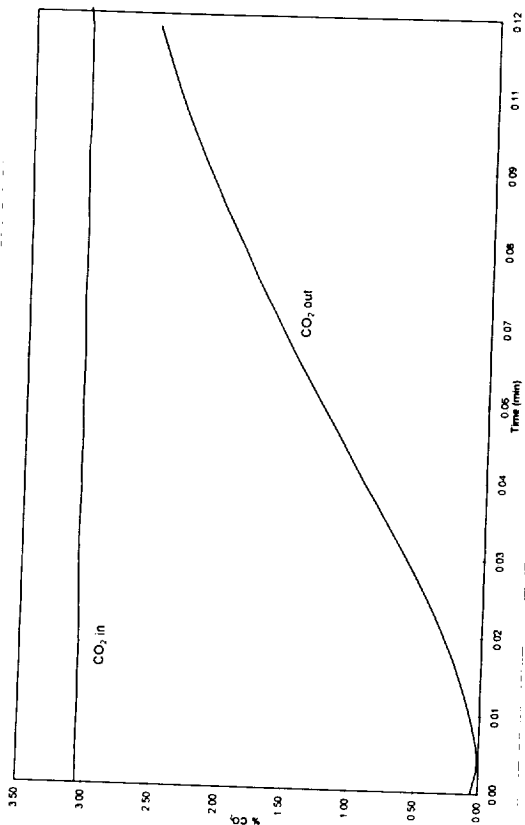
a. CO₂ Removal FCMS
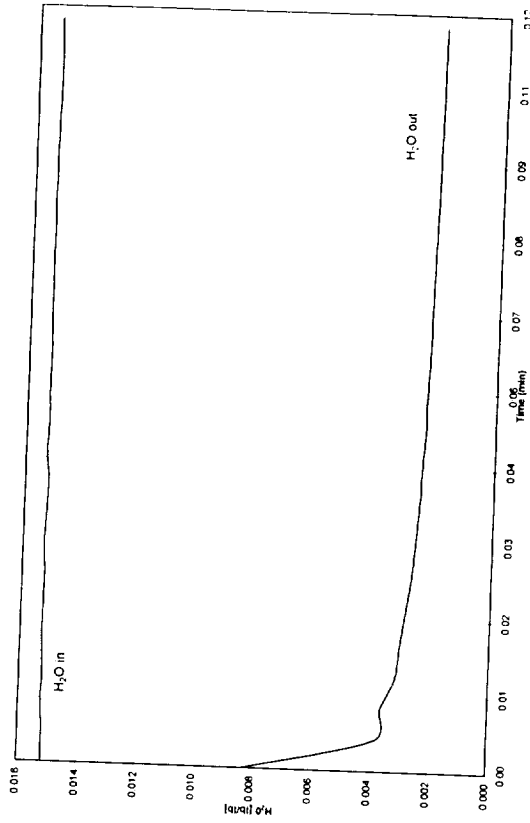
b. CO₂ Removal Zeolite
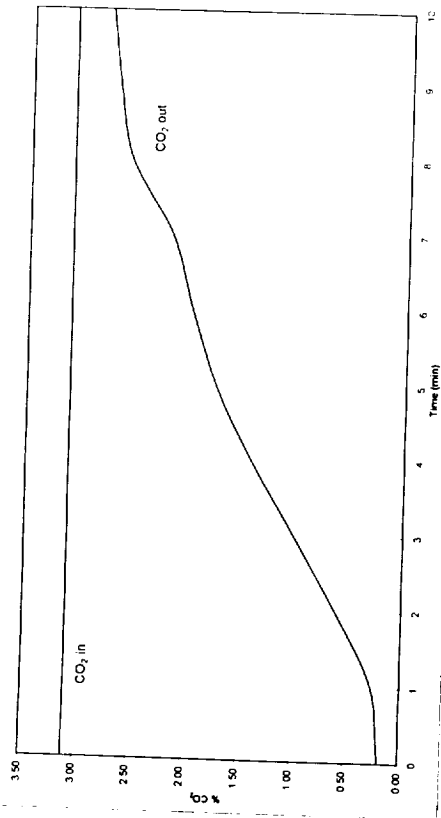
c. H₂O Removal FCMS
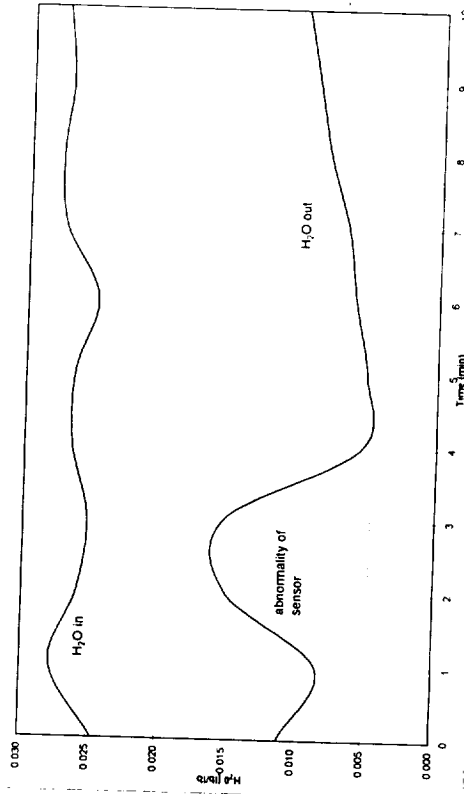
d. H₂O Removal Zeolite

Figure 5-1. Breakthrough at Suit Conditions
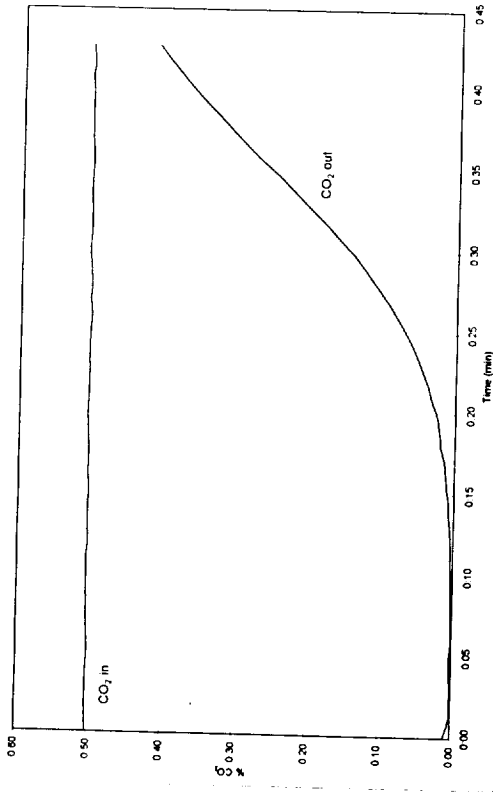
a. CO_2 Removal FCMS
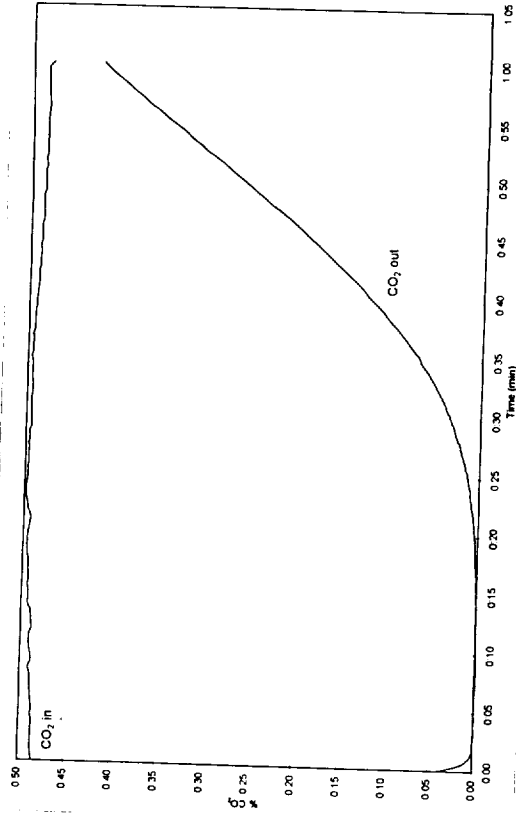
b. CO_2 Removal Zeolite
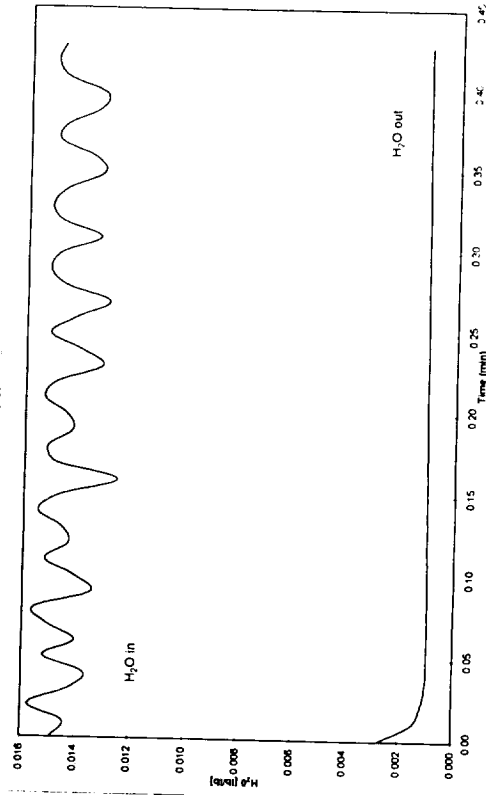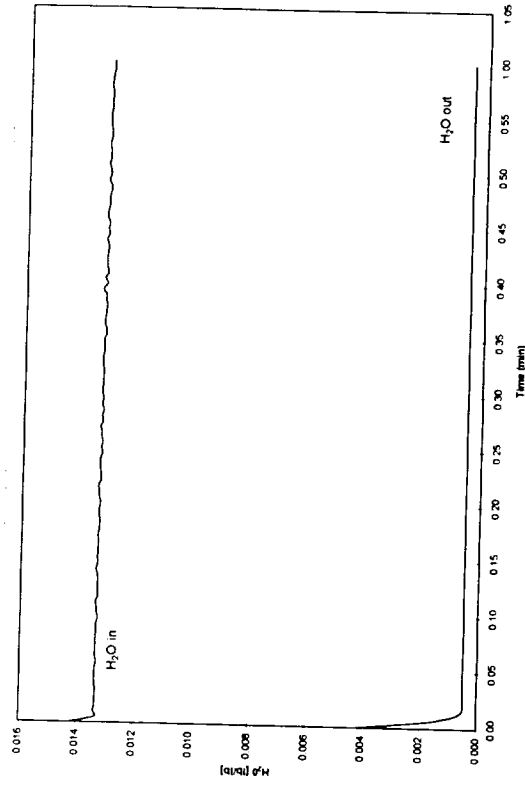
c. H_2O Removal FCMS

d. H_2O Removal Zeolite

Figure 5-2. Breakthrough at Station Conditions

AlliedSignal
AEROSPACE

Aerospace Equipment Systems
Torrance

97-69288
Page 5-3

TABLE 5-2				
CYCLIC SUMMARY DATA				
	Suit		Station	
	FCMS	Zeolite	FCMS	Zeolite
First half-cycle:				
CO_2 removal efficiency, percent	70	93	93	97
Removal rate, lb/hr	0.15	0.21	0.023	0.024
Steady state (final half-cycle):				
CO_2 removal efficiency, percent	35	41	80	64
CO_2 removal rate, lb/hr	0.093	0.1	0.021	0.015
Water removal efficiency, percent	75	87	94	96
Water removal rate, lb/hr	0.11	0.08	0.034	0.037

5.3 THERMAL AND KINETIC TESTS

More thorough investigations of the key design and operational characteristics were made. Specifically, the following were investigated:

- The performance of an isothermal or thermally coupled bed as compared to an adiabatic bed

- The effects of residence time and superficial velocity on performance

- Operations — air save

5.3.1 Bed Design (Thermal Effects)

Thermal effects in an adsorption system will have a large impact on the performance. The adsorption process is exothermic; as the sorbent takes up CO_2 or water, the sorbent temperature rises. However, the capacity of the sorbent is reduced at higher temperatures. The inverse is true during desorption — the sorbent tends to cool off, which slows down the release of CO_2.

Early testing showed that the adiabatic bed performed poorly, mainly due to high temperatures reached in the bed. During the adsorption half-cycle, the bed reached regeneration temperatures (approximately 120°F), which significantly reduced the capacity of the material. By thermally coupling the two half-cycles to allow some of the heat of reaction to warm the desorbing material and the cooler desorbing material to be exposed to vacuum, the adsorbing side, was cooled. A significant performance gain was achieved using this approach. Tests were performed to determine the efficiency of the thermally coupled bed. Comparing two test runs at space station conditions (see Table 5-3), the improved performance of the thermally coupled bed over the adiabatic bed is apparent.
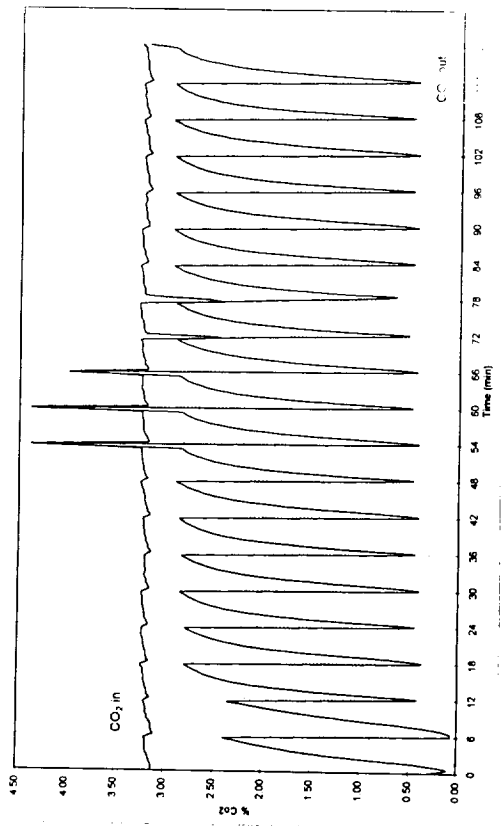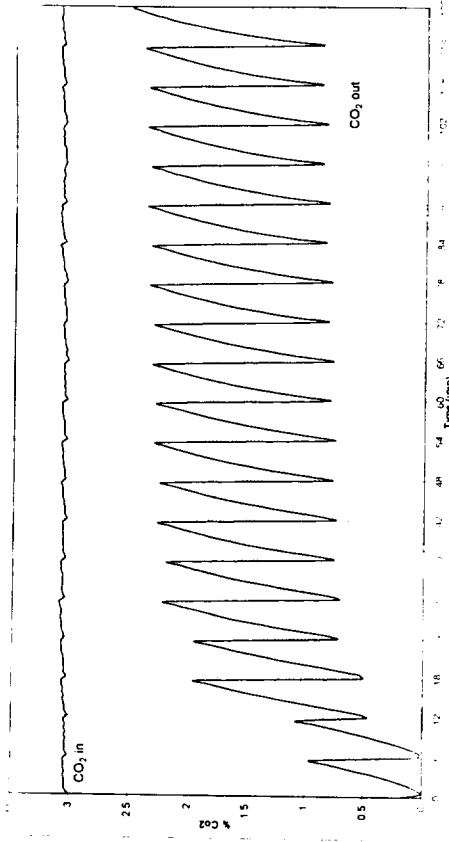
b. CO₂ Removal Zeolite
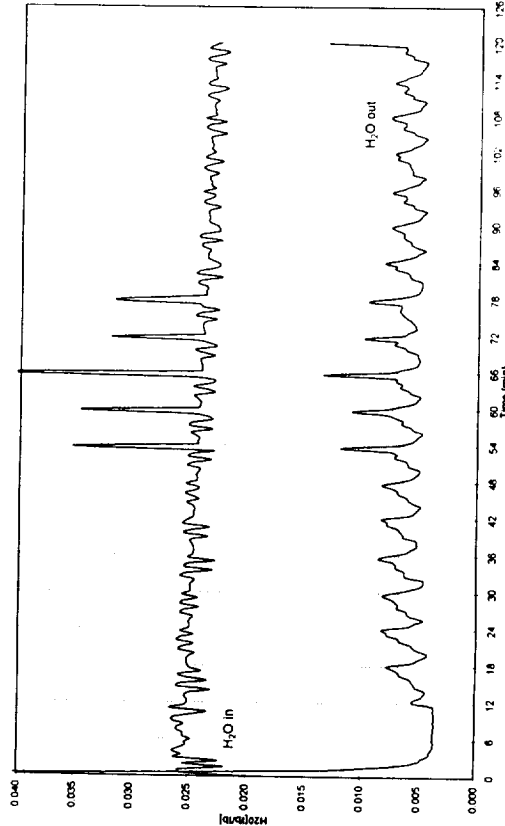
d. H₂O Removal Zeolite
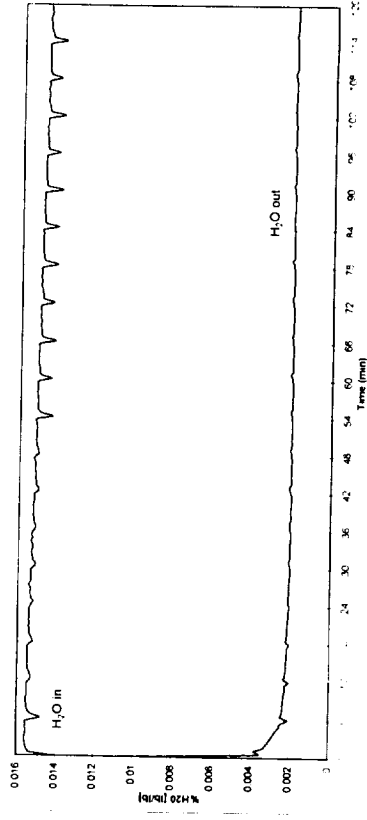
a. CO₂ Removal FCMS

c. H₂O Removal FCMS

Figure 5-3. Cyclic Data at Suit Conditions (6 Min Adsorb/Desorb)
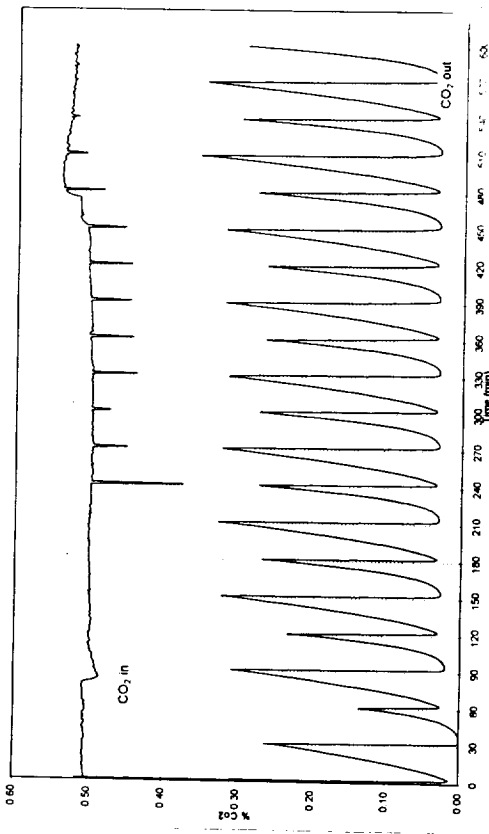
a. CO₂ Removal FCMS
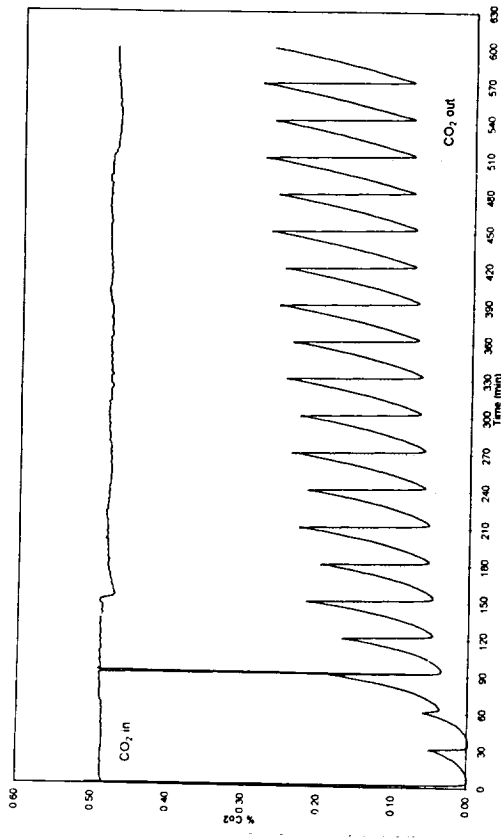
b. CO₂ Removal Zeolite
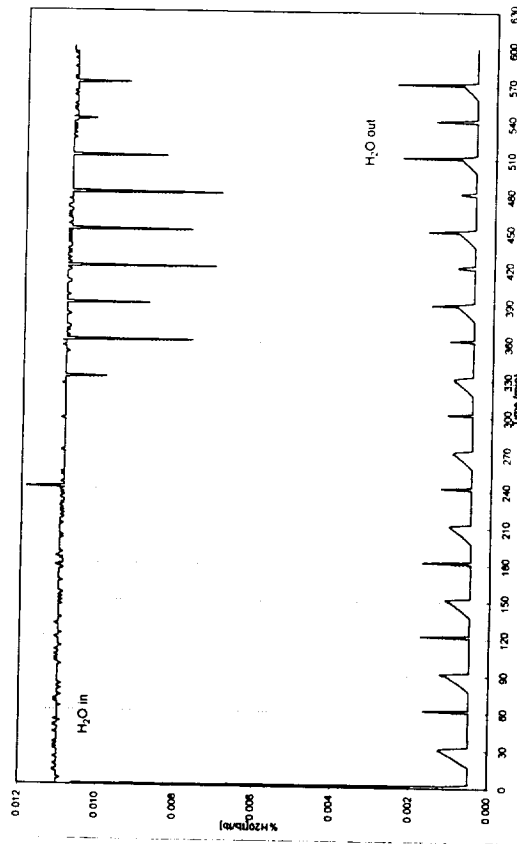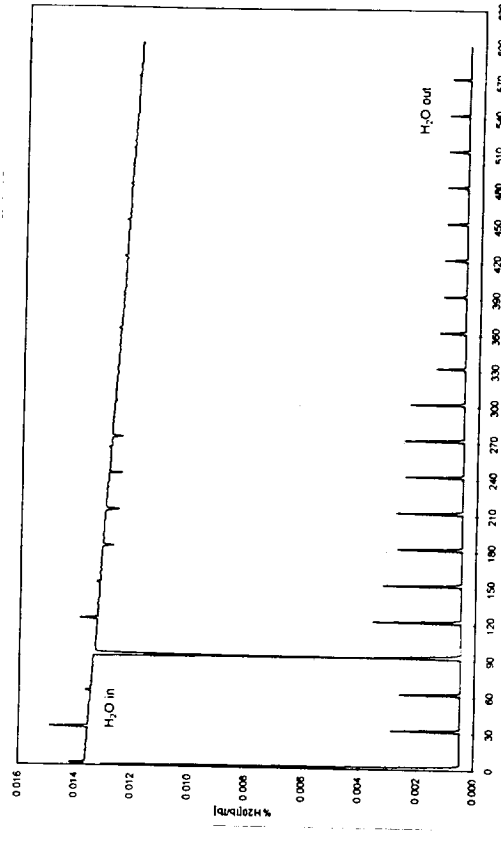
c. H₂O Removal FCMS

d. H₂O Removal Zeolite

Figure 5-4. Cyclic Data at Station Conditions (30-min Adsorb/Desorb)

AlliedSignal
AEROSPACE
Aerospace Equipment Systems
Torrance

97-69288
Page 5-6

TABLE 5-3

FCMS CYCLIC TEST (STATION CONDITIONS)

	Thermally coupled	Adiabatic
Regenerated removal of CO_2, percent	93	56
Steady-state removal of CO_2, percent	80	26
Amount of CO_2 at inlet, lb/hr	0.0270	0.0278
Amount of CO_2 removed (steady state), lb/hr	0.0218	0.0072
Steady-state H_2O removal, percent	95	84
Steady-state H_2O at inlet, lb/hr	0.0364	0.0369
Steady-state H_2O removal, lb/hr	0.0346	0.0310
Air in/out delta temp., $\Delta°F$	6	15
Local material delta temp., $\Delta°F$	10	50

Thermally coupled performance was also compared with an isothermal test bed representing the theoretical best case, at two differing temperatures and at suit conditions. The isothermal test involved flowing hot water through one of two sides of the bed at a rate of 1.78 gal/min. The temperature was controlled with a cooling cart; two temperatures of 70°F and 90°F were run. Table 5-4 shows the performance results of each.

The thermally coupled bed was slightly hotter than the 70°F isothermal test on the adsorption side; however, the steady-state CO_2 removal and H_2O removal performance was very similar. The 90°F isothermal test did show a slight degradation in performance compared with the other two tests. This is a good indication that the thermal coupling approach is nearly as effective as the use of a constant temperature source for this bed design.

5.3.2 Residence Time and Superficial Velocity

Residence time and superficial velocity are determined by the bed dimensions for a given flow rate and have a significant impact on the performance, both total capacity and dynamic efficiency (as measured by the percent CO_2 removal at any given time after desorption). An initial comparison between bench and full-scale tests showed that the performance in a packed bed is improved with a longer residence time and a lower superficial velocity.

A more detailed investigation into the impact of these two variables at representative conditions was performed.

TABLE 5-4

FCMS CYCLIC TEST (SUIT CONDITIONS)

	Thermally coupled	Isothermal	Hot Isothermal
Regenerated removal of CO_2, percent	70	75	58
Steady-state removal of CO_2, percent	35	35	36
Amount of CO_2 at inlet, lb/hr	0.270	0.280	0.25
Amount of CO_2 removed (steady-state), lb/hr	0.093	101	0.087
Steady-state H_2O removal, percent	75	72	65
Steady-state H_2O at inlet, lb/hr	0.109	0.123	0.118
Steady-state H_2O removal, lb/hr	0.082	0.089	0.087
Air in/out delta temp., $\Delta°F$	5	3	10
Local material delta temp. (max. at bed center), $\Delta°F$	28	25	25*
*Nominal temperature was elevated by 20°F			

Three variations of the test bed were used (Figure 5-5):

(a)   The isothermal test bed as designed

(b)   The isothermal test bed with the same flow length and approximately 60 percent of the face area (60 percent sorbent volume)

(c)   The isothermal test bed with the same face area and 50 percent of the flow length (50 percent sorbent volume)

Figure 5-6 shows the impact of varying the residence time at constant superficial velocity, Figure 5-7 the impact of varying superficial velocity at a constant residence time. For the operational conditions investigated, the residence time has a larger impact on both CO_2 and water adsorption than the superficial velocity. This effect is more pronounced for CO_2 than water.

5.3.3   Air Save

Pressure-swing regeneration was originally chosen for investigation because it presents the potential for an in-place regenerable CO_2 removal system with lower power than the more conventional heat-regenerated sorbents. This reduction in power is particularly interesting if the vacuum of space is used to regenerate the bed. A drawback to such a system, however, is that there is a gas loss associated with each half-cycle corresponding to the ullage and the gases adsorbed by the sorbent.

		TEST ARTICLE		1/2 HEIGHT		1/2 FLOW LENGTH
VOLUME (V)	=	HWL	=	$\dfrac{HWL}{2}$	=	$\dfrac{HWL}{2}$
VOLUMETRIC FLOW (F)	=	F	=	F	=	F
FACE AREA (A)	=	WH	=	$\dfrac{WH}{2}$	=	WH
RESIDENCE TIME (RT)	=	$\dfrac{WHL}{F}$	=	$\dfrac{WHL}{2F}$	=	$\dfrac{WHL}{2F}$
SUPERFICIAL VELOCITY	=	$\dfrac{F}{WH}$	=	$\dfrac{2F}{WH}$	=	$\dfrac{F}{WH}$
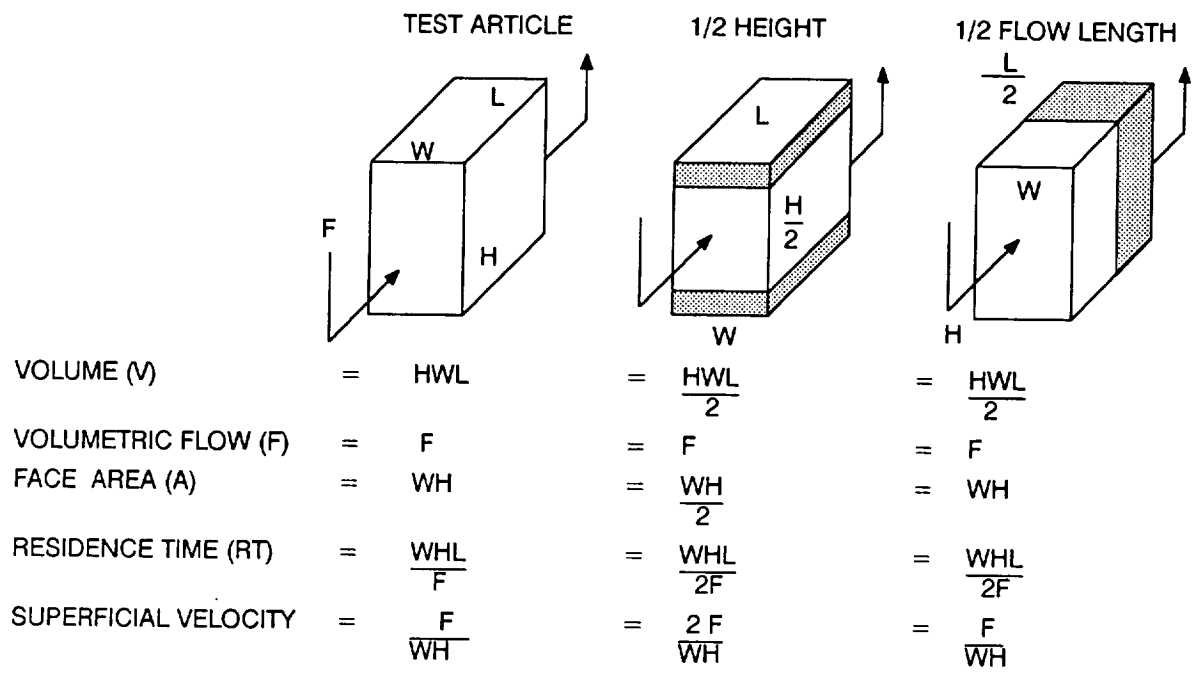
IG–31043

Figure 5-5. Sieve/Bed Geometry (Variation of Aspect Ratio)
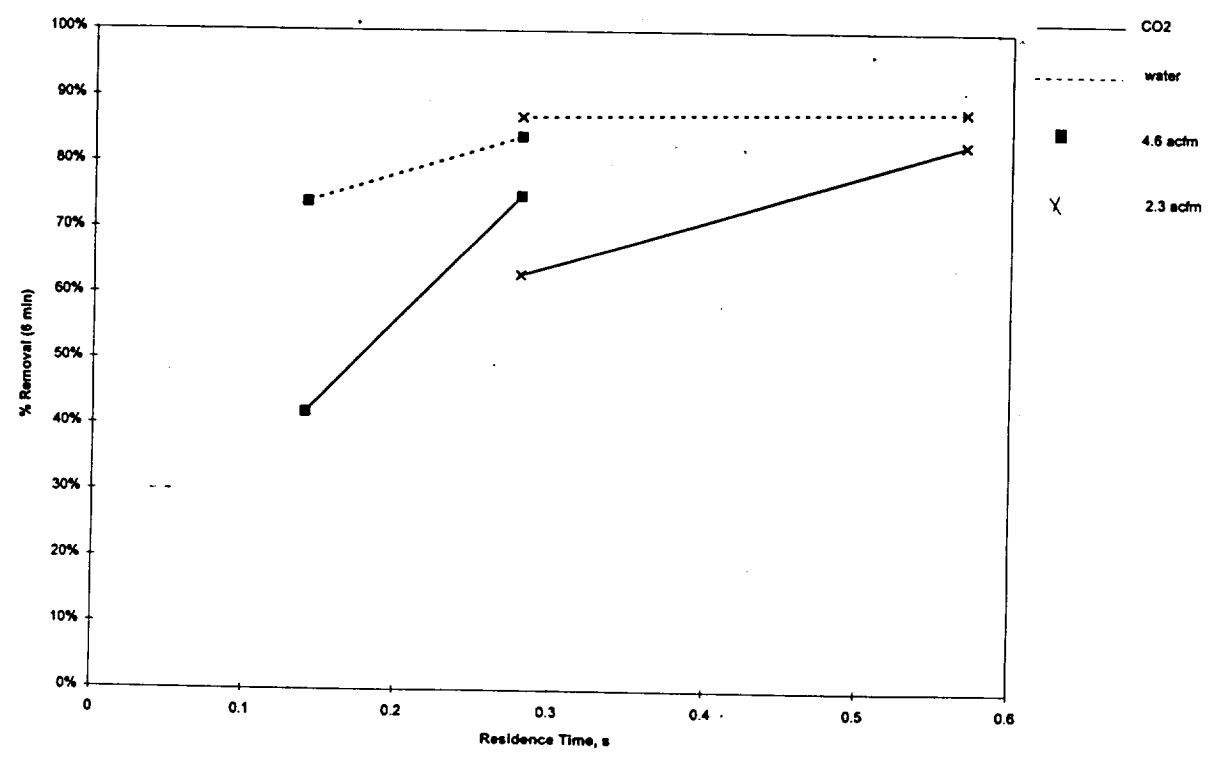
Figure 5-6. Aspect Ratio Effect on Residence Time
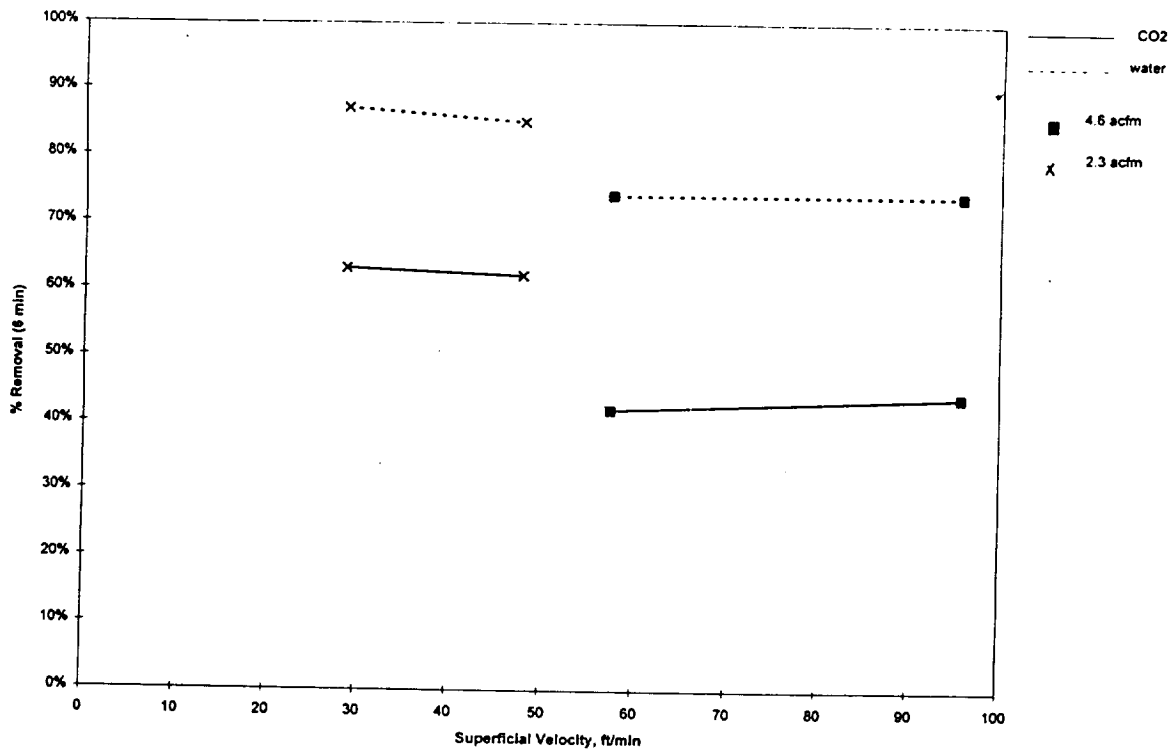
Figure 5-7. Aspect Ratio Effect on Superficial Velocity

One approach to reducing the gas loss is to allow the bed at system pressure to be exposed to the bed at vacuum (closing all other ports) and allowing the pressure between the two beds to stabilize. This saves approximately one-half of the air that normally would have been lost to vacuum, and would bring the scrubbed bed up to a pressure level closer to the system pressure before exposing it to the air loop for adsorption. This concept was tested by allowing the two beds to "cross-talk" for approximately 2 sec during valve switching. An additional valve was added to the test rig to allow the process air to bypass the beds and return to the air loop during the equalization period. The testing showed that the performance was identical to a system without air save, and the 2-sec stabilization period was adequate for the beds to stabilize. At a 2-sec CO_2 removal "downtime" for the given flow rate, estimations indicate that the increase in CO_2 concentration is negligible, even in a closed-loop system.

6. PERFORMANCE COMPUTER MODEL

Computer modeling was performed using a FORTRAN code developed for NASA and utilized for several programs, including the CO_2 removal systems on Skylab and the space station. The model was constructed initially to predict the transient performance of adsorption and desorption where CO_2 and H_2O were removed by separate adsorbent materials. The model simulates thermal-assisted pressure-swing performance for an adiabatic zeolite test bed. The model was upgraded to simulate the FCMS sorbents in an isothermal pressure-swing system.

FCMS sorbent characteristic data and thermal profiles of the sorbent bed from performance test were both input into the model, which was then evaluated against actual adiabatic test data.

When the adiabatic model was proven to predict test data relatively well, the model was extended to simulate isothermal test. These data were also evaluated against actual test data and showed good correlation. The model can be used as a tool for predicting performance over a range of conditions and operation protocol.

6.1 ADIABATIC OPERATION (CO_2 ONLY)

Laboratory data were collected for adsorption/desorption of CO_2 from air at atmospheric pressure and compared with model results. The adiabatic bed contained FCMS-X28. CO_2 isotherm data were input after fitting AlliedSignal data to a Unilan-type equation for adsorption.

Figure 6-1 shows the comparison of model and experimental results for a breakthrough curve, showing relatively good agreement. Figure 6-2 shows the comparison of the same system over ten 6-min half-cycles. The general shapes of the outlet CO_2 concentrations are good; however, initial cycles of the laboratory data show shifting upwards with time indicating residual CO_2 in the bed until steady-state is reached.

6.2 THERMALLY COUPLED OPERATION (CO_2/H_2O)

The model results were compared to results from test of a thermally coupled bed. The approach is to model one of a total of 63 channels (63 channels adsorbing, 63 desorbing); flows are assumed equally divided among the 63 channels. The model was set up to have 20 nodes from inlet to outlet. The experimental data used to compare results came from a 3/14/97 run made with FCMS-X28. The CO_2 isotherm came from AlliedSignal FCMS patent and other bench-top tests; for H_2O, silica gel was used as the isotherm as no separate H_2O isotherm data for FCMS were available. The 20 nodes are broken into two sections: the first ten were set for H_2O removal and the second ten were set for CO_2 removal. The H_2O nodes used silica gel with isotherm data extracted from data previously input in the model by others; the CO_2 nodes used FCMS-X28 data.

In modeling the thermally coupled reactor, a cooling/heating fluid that removes or gives heat to each node was used. An arbitrarily high quantity of fluid was assumed such that the reactor core temperature correlates with the laboratory data (-80°F).
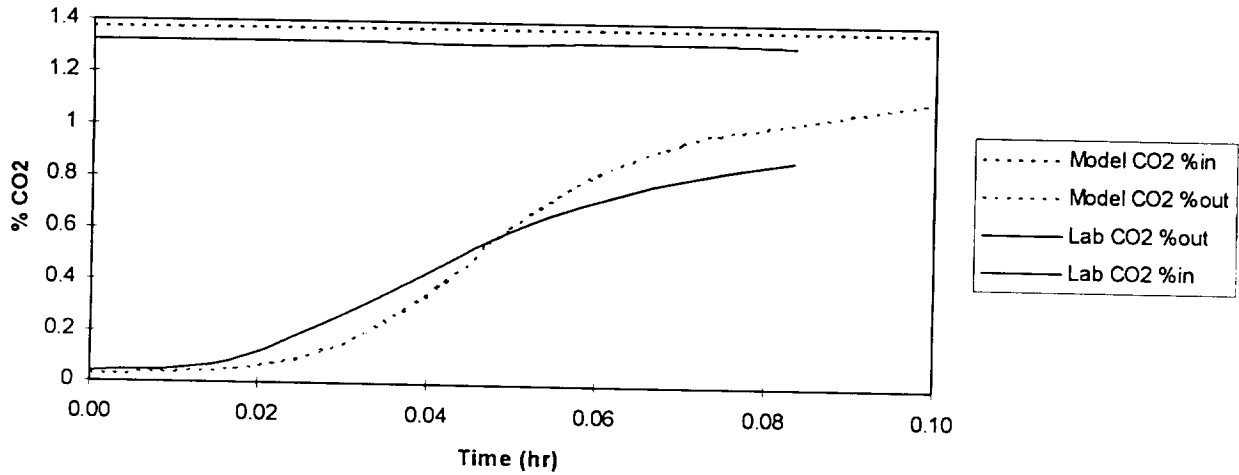
Figure 6-1. Model and Laboratory Curves for Adiabatic CO_2 Removal (80 Percent Breakthrough)
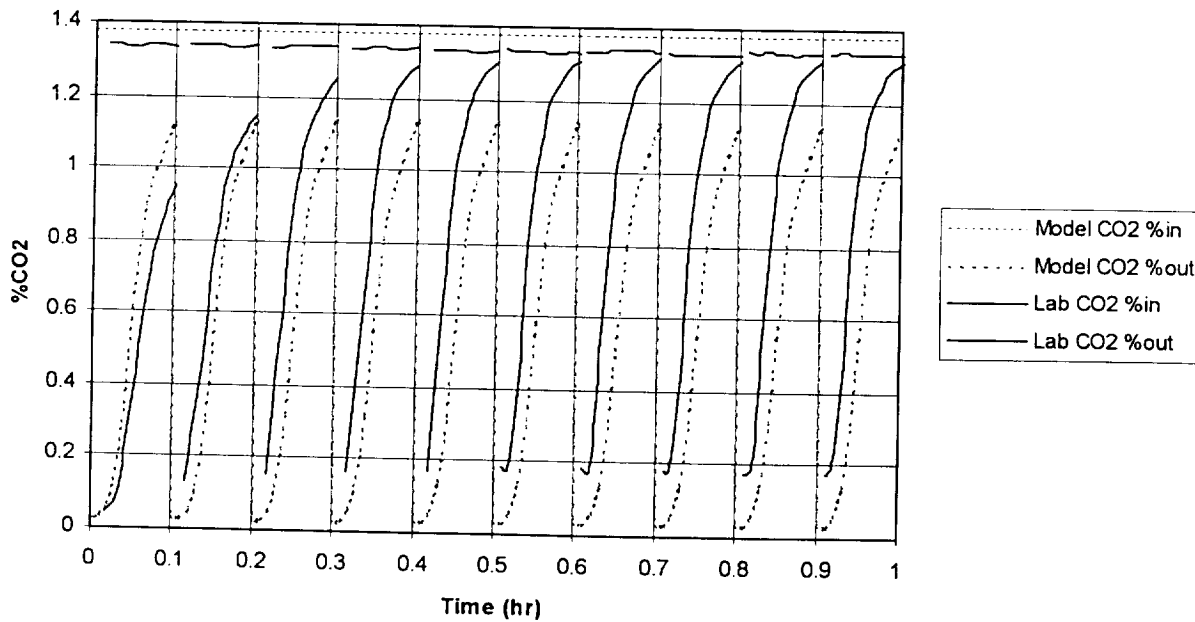
Figure 6-2. Model and Laboratory Results for Adiabatic CO_2 Removal (Ten Cycles)

Figures 6-3 and 6-4 show a comparison of CO_2 and H_2O volume percent in/out, respectively, for the laboratory and model runs. The CO_2 shows a decent match. The H_2O for the model predicts about two times that of the laboratory data by the tenth cycle (t = 1 hr) in terms of percent H_2O out. This difference is caused by the estimation of FCMS-X28 water capacity by that of silica gal.

6.3 THERMALLY COUPLED CO_2/H_2O PERFORMANCE STUDY

The model was used to extrapolate the performance of a thermally coupled design that could be used for a regenerable portable life support system.

The model predicts averaged removal rates for this model size of 0.132 and 0.209 lb/hr CO_2 and H_2O, respectively, at the end of the tenth cycle. The CO_2 and H_2O removal rates at the end of the first cycle were 0.197 and 0.246, respectively. The removal percentages after this first cycle are 79 and 96 percent respectively. After the tenth cycle, the removal percentages have been lowered to 53 and 81 percent, respectively, as the residual weight fraction of CO_2 and H_2O in the adsorbent bed increases over time. Based on previous test experience, these data seem reasonable and indicate that the model is a useful design tool.
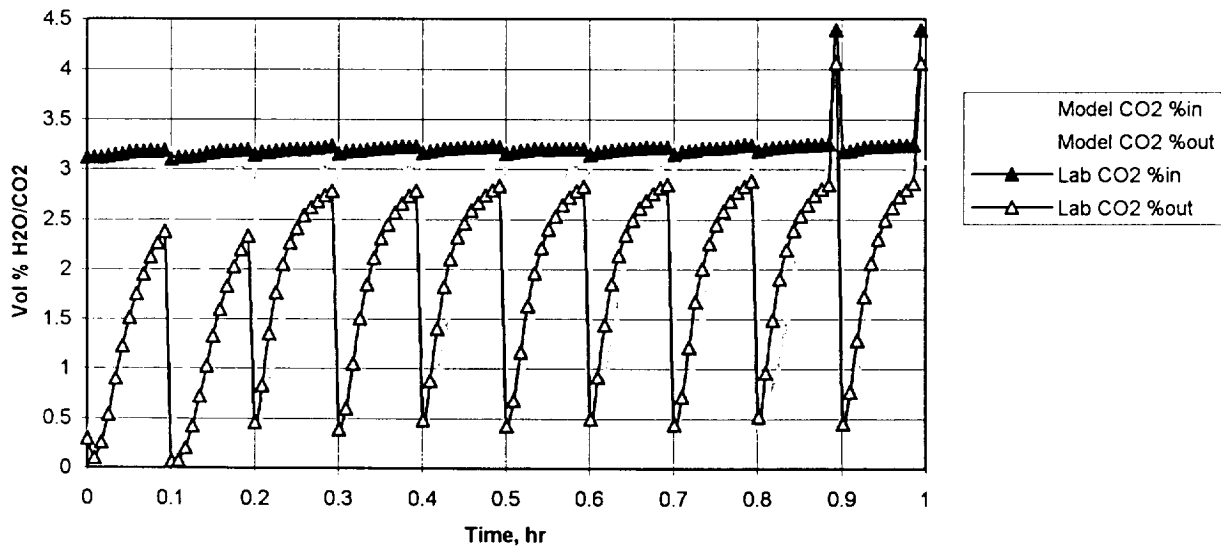
Figure 6-3.   Thermally Coupled Model and Laboratory
Results for FCMS-X28 CO_2 Removal
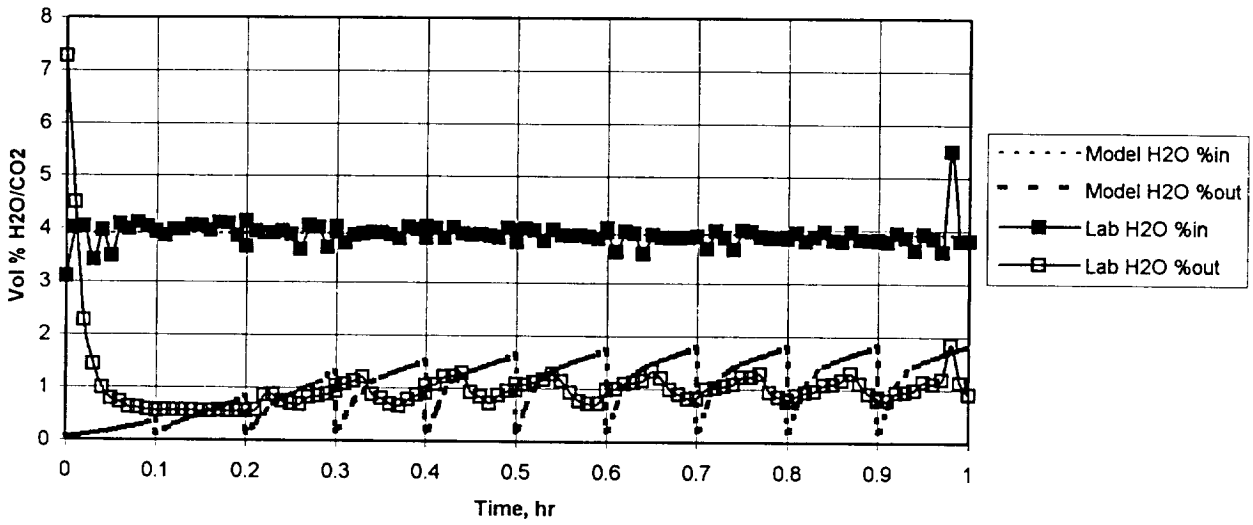
Figure 6-4. Thermally Coupled Model and Laboratory
Results for FCMS-X28 H_2O Removal

AlliedSignal
AEROSPACE

Aerospace Equipment Systems
Torrance

97-69288
Page 6-4

7. SYSTEM STUDIES

The data obtained over the course of this study were used to develop system concepts for both spacesuit and multiperson applications, such as space station.

The majority of this effort focused on the FCMS sorbent, which was selected for the following reasons:

- The FCMS can be completely regenerated in a pressure-swing system.

- The heat of regeneration for FCMS is considerably lower than that of the molecular sieves; thus, in a heat-assisted pressure-swing system, the FCMS has lower power requirements.

- The FCMS CO_2 removal is essentially unaffected by the presence - or lack - of humidity in the airstream

System concepts were compared against current technologies using mass, volume, power, consumables, safety, and reliability as parameters of comparison.

7.1 SPACESUIT CO_2 REMOVAL

The three spacesuit CO_2 removal systems that are compared in this study are (1) the current U.S. EMU, which uses LiOH cartridges; (2) a metal oxide CO_2 removal system being developed for the International Space Station EMU; and (3) a two-bed pressure-swing system. Table 7-1 presents a summary of the tradeoff based on the key performance parameters for each system. The table shows the following:

(a)   The LiOH system has the lowest on-suit weight and is the simplest and most robust system. Its logistics, however, are unattractive; it requires a new LiOH canister for each EVA, and the consumables mass thus grows proportionally with the number of EVA's.

(b)   The metal oxide system is fully regenerable, is relatively small, and requires only low power on the spacesuit. However, this system requires a high-power, high-temperature regeneration system.

(c)   The pressure-swing system has comparable on-suit mass and volume as the metal oxide system with the advantages of:

-   In-place regeneration requiring no additional regeneration hardware. The power required per EVA is only 1.1 percent of that required by the metal oxide system.

-   Unlimited EVA duration.

-   Long operational life.

TABLE 7-1

SUMMARY OF PERFORMANCE PARAMETERS FOR SPACESUIT CO₂ REMOVAL TECHNOLOGIES

	LiOH (EMU)	Metal Oxide	Two-Bed Pressure Swing
Technique	Disposable sorbent cartridge	Sorbent cartridge with thermal regeneration	Sorbent canister with in-place pressure-swing regeneration.
Sorbent	LiOH	Silver oxide + hygroscopic catalyst	Functionalized carbon molecular sieve
System mass on suit, kg	3.2	13.6	7.4
System volume, m³	0.0065	0.0065	0.0084
Max. duration per EVA, hr	7 (103 kg CO_2/m³)	8 (304 kg CO_2/m³)	Unlimited
Power per EVA, w-hr	Low power required to cool the system	6000 w-hr for regeneration*	0.66
Consumables, kg/EVA	CO_2 and trace gases removed + ullage + 3.2 kg LiOH cartridge	CO_2 and trace gases removed + ullage	CO_2, water, and trace gases removed + ullage
H_2O removal rate, kg/hr	0	0.136 (1.09 kg in 8 hours)	0.068
CO_2 sorbent rate, kg/hr	0.096	0.091	0.091
System average pressure drop, kPa	0.249 (1.0 in. H_2O)	0.107 (0.8 mm Hg)	0.124 (0.5 in. H_2O)
Operational life, #EVA	1	> 101	> 500
Activity between EVA	Remove and replace cartridge	Remove cartridge and regenerate (12 hr)	None
Support hardware mass, kg	Storage of cartridges for entire duration	44.45*	0
Support Hardware Volume, m³	0	0.17*	0
Safety and reliability	Highly safe and reliable: - No moving parts - Proven technology	Safe and reliable on suit: - No moving parts on suit - High temperature only between EVA - Some material lifetime issues to be resolved	Safe and reliable: - Shutoff valve - Proven valve technology - Manual override - Two sorbent beds
References	SAE-961484	SAE-961484 SAE-921289 *SAE-9567657	Contract NAS9-19607 and test data presented in this report

7.2 STATION APPLICATIONS

The station application differs from the spacesuit primarily in the following:

- Total pressure: 1 atmosphere versus a reduced pressure

- Continuous operation over an extended duration as compared to a short, 4 to 8 hr, EVA.

- Load/sizing: Several persons versus one person

Comparing the space station CDRA to a two-bed pressure swing system (Table 7-2) shows that the pressure-swing system is 40 percent lighter, requires half the volume, and utilizes less than 30 percent of the power required by CDRA. The pressure-swing system has the disadvantage of a higher gas loss than CDRA corresponding to the water removed.

TABLE 7-2

VEHICLE CO_2 REMOVAL SYSTEMS

	Carbon Dioxide Removal Assembly (CDRA)	Two-Bed Pressure Swing
Vehicle	Space Station (U.S. lab rack)	Station
Technique	Four-bed molecular sieve heat and vacuum regeneration.	Sorbent regenerable by pressure swing
Sorbent(s) - CO_2/water	Silica gel/zeolite 13X and zeolite 5A	FCMS
Load, # crew	4 to 6	4 to 6
System mass, kg	195	117
System volume, m	0.486	0.243
Flow rate,kg/hr	40.8	46
Max. duration (lifetime), hr	20 year	20 year
Average cycle power, w	743*	200
Consumables, kg/wk	Ullage (negligible) + CO_2 adsorbed	Ullage (negligible) + CO_2 and water adsorbed
H_2O removal rate, kg/hr	0	0.40
CO_2 sorbent rate, kg/hr	0.34	0.34
References	SAE-961519, SAE-941396, SAE-972419	Test data presented in this report.
*High-voltage day-night average		

8. BIBLIOGRAPHY

Boehm, A. M., G. F. Allen, P. J. Chen, D. L. Sandersfeld, "Orbiter Regenerable CO_2 Sorbent Life Characterization," SAE-972264, July 1997.

Buchmann, O. A., A. K. Macknight, D. Gomez, L. N. Supra, "Development of a Regenerable Metal Oxide CO_2 Absorber for EMU Applications," SAE-961483, July 8, 1996.

Butler, L. B., Jr., J. J. Freszcza, G. A. Thomas, "Development Status of the Metal Oxide Regenerable CO_2 Removal System for the NASA EMU," SAE-972505, July 1997.

Davis, S. H. and L. D. Kissinger, "CO_2 and Humidity Removal System for Extended Shuttle Missions: Equilibrium Testing and Performance Analysis," ICES, July 12, 1976.

Filbum, R., T. A. Nalette, T. P. Hamilton, J. Cusick, "Development of a Regenerable Metal Oxide Sheet Matrix CO_2 Removal System," SAE-921298, July 13, 1992

Filburn, T., T. Nalette, J. Genovese, G. A. Thomas, "Advanced Regenerable CO_2 Removal Technologies Applicable to Future EMU's," SAE-961484, July 8, 1996.

Fraas, A. P., M. N. Ozisik, Heat Exchanger Design, John Wiley & Sons, New York, 1965.

Graft J., S. Tongue, T. Tilburn, E. Taddey, "Orbiter Upgrade Activities for a Fail Safe Regenerative CO_2 Removal System," SAE-972265.

Hart, J. M., J. B. Borghese, C. H. Chang, R. J. Cusick, "Portable Life Support System Regenerative CO_2 and Water Vapor Removal by Metal Oxide Absorbents Preprototype Hardware Development and Testing," SAE-921299, July 13, 1992

Hwang, K. C., A Transient Performance Method for CO_2 Removal with Regenerable Adsorbents, NASA Document 72-8786.

Jacobs, P., P. G. Paul, P. H. M. Feron, C. J. Savage, and J. Witt, "Integrated CO_2 and Humidity Control by Membrane Gas Absorption," SAE-972560, July 1997.

Kimble, M. C., M. S. Nacheff-Benedict, L. A. Dall-Bauman, M. R. Kallberg, "Molecular Sieve CO_2 Removal Systems for Future Missions: Test Results and Alternative Designs," SAE-941396, July 20, 1994.

Kuznetz, L. H., O. Gwynne, "Spacesuits and Life Support Systems for the Exploration of Mars," Journal of the British Interplanetary Society, Vol. 45.

Lee, M. C., M. Sudar, P. S. Beckstrom, R. J. Cusick, "Electrochemically Regenerable Metallic CO_2 and Moisture Control System for an Advanced EMU Application," SAE-881061, July 11, 1988.

Mudoch, K. E. , G. A. Thomas, B. Duffield, "Venting Membrane for EVA CO_2 and H_2O Removal," SAE-972504, July 1997.

Nalette, J, T. Nalette, "Life Characterization of Enhanced Solid Amine CO_2 Sorbents," SAE-941395, June 20, 1994.

Ouellette, F. A., G. Allen, G. S. Baker, D. J. Woods, "Development and Flight Status Report on the Extended Duration Orbiter Regenerable Carbon Dioxide Removal System," SAE-932294, July 12, 1993.

Perry, J. L., R. L. Carrasquillo, G. D. Franks, K. R. Frederick, J. C. Knox, D. A. Long, K. Y. Ogle, and K. J. Parris, "International Space Station Integrated Atmosphere Revitalization Subsystem Testing," SAE-961519, July 8, 1996.

Severin, G. I., I. P. Abramov, V. I. Svertshek, A. Yu. Stoklisky, "Some Results on Modification of the EVA Suit for the MIR Orbiting Station," SAE-951550, July 10, 1995

Supra, L. N., S. F. Brasseaux, "Molecular Sieve CO_2 Removal Systems: International Space Station and Lunar-Mars Life Support Test Project," SAE-972419.

Valenzuela, D., A. Myers, Adsorption Equilibrium Data Handbook, Prentice-Hall, 1989.

Von Jouanne, R. G., R. S. Baker, "Detailed Integration Analysis of the Space Station Life Support System," SAE-941510, June 20, 1994.

Zaitsev, E. N., A. S. Guzenberg, A. M. Riabkin, T. K. Shirokova, "Gas Composition Support Aids for Space Vehicle Compartments Based on CO_2 Hydrogenation, H_2O Electrolysis, CO_2 Removal and Concentration," SAE-951542, July 10, 1995

Zinners, H. A., A. R. Oroskar, C. H. Chang, Carbon Dioxide Removal Using Animated Carbon Moles.

Flammability, Odor, Offgassing, and Compatibility Requirements and Test Procedures for Materials in Environments that Support Combustion, NHB 8060.1c, April, 1991.

Regenerable Metal Oxide Based Extravehicular Mobility Unit Atmospheric Control System, AlliedSignal Document 95-67657-14, October 31, 1995.

Space Biology and Medicine II Life Support and Habitability, published and distributed by AIAA/Nauka Press, Washington, DC/Moscow

Spacesuit CO_2/H_2O Removal and Regeneration System (Scores), AlliedSignal Document 97-69041, March 3, 1997.

Specification/Statement of Work for a Regenerable Metal Oxide Based Extravehicular Mobility Unit Atmospheric Control System, 9BP-09-5-13P, Section C.

Standard Test Method for Total Mass Loss and Collected Volatile Condensable Materials from Outgassing in a Vacuum Environment, ASTM E 595-93, June 15, 1993.

Statement of Work for a Space Suit CO_2/H_2O Removal and Regeneration System, Contract for NASA JSC NAS 9-19607.

Structural Design and Verification Requirements, SSP30559, Rev. B, June 30, 1994.

"The Experience in Operation and Improving the Orlan-Type Space Suits," J. P. Abramov, Acta Astronautical, Vol. 36, No. 1, pp 1-12, 1995

Carbon Dioxide Removal Using Aminated Carbon Molecules, Patent 4,810,266 (March 7, 1989), H. A. Zinner, A. R. Oroskar, C. H. Chang, AlliedSignal Aerospace.

APPENDIX

TEST MATRIX

			APPENDIX				
			TEST MATRIX, FIRST YEAR				

Test ID	Date	Bed ID	Adsorbent Type	Inlet CO$_2$ Conc., % vol	Inlet H$_2$O Vap. Pressure, psia	Airflow, lb/hr	Half-Cycle Time, min
SAT-1	12-Jun	KB3	5A	1	Dry	4.34	NA
SAT-2	13-Jun	KB4	5A	1	Dry	4.34	NA
SAT-3	22-Jul	BD15	5A and 13X	1	Dry	5.16	NA
SAT-4	22-Jul	BD16	5A and 13X	1	Dry	5.16	NA
SAT-5	23-Jul	BD15	5A and 13X	1	Humid	5.1744	NA
SAT-6	23-Jul	BD16	5A and 13X	1	Humid	2.74	NA
SAT-7	24-Jul	RM17	5A and 13X	1	Dry	5.1072	NA
SAT-8	24-Jul	RM17	5A and 13X	1	Humid	5.1774	NA
SAT-9	25-Jul	RM17	5A and 13X	1	Humid	2.7774	NA
SAT-10	1-Aug	KB18	5A and 13X	1	Dry	19.62	NA
SAT-11	2-Aug	KA20	5A and 13X	1	Humid	5.3862	NA
SAT-12	5-Aug	KA20	5A and 13X	1	Humid	5.1	NA
SAT-13	6-Aug	KB21	5A and 13X	1	Dry	5.2278	NA
SAT-14	6-Aug	KB18	5A and 13X	1	Dry	5.2278	NA
SAT-15	7-Aug	KB21	5A and 13X	1	Humid	5.0928	NA
SAT-16	7-Aug	KA20	5A and 13X	1	Dry	5.031	NA
SAT-17	7-Aug	KB18	5A and 13X	1	Dry	5.031	NA
SAT-18	8-Aug	KB22	5A and 13X	1	Dry	5.227	NA
DES-1	11-Jul	KB13	5A	1	Dry	5	NA
DES-2	20-Jun	KB4	5A	1	Dry	7.422	NA
DES-3	20-Jun	KB5	5A	1	Dry	7.422	NA
PSA-1A	12-Jul	KB13	5A	1	Dry	5	10
PSA-1B	12-Jul	KB14	5A	1	Dry	5	10
PSA-2A	17-Jul	KB13	5A	1	Dry	5	20
PSA-2B	17-Jul	KB14	5A	1	Dry	5	20
PSA-3A	19-Jul	KB13	5A	0.4	Dry	5	10
PSA-3B	19-Jul	KB14	5A	0.4	Dry	5	10
PSA-4A	26-Jul	KB18	5A and 13X	1	0.36	5.1774	10
PSA-4B	26-Jul	RM17	5A and 13X	1	0.36	5.1774	10
PSA-5A	27-Jul	KB18	5A and 13X	1	0.31	15.06	10
PSA-6A	29-Jul	KB18	5A and 13X	1	0.3	10	10
PSA-6B	29-Jul	KB19	FCMS	1	0.3	10	10
PSA-7A	31-Jul	KB18	5A and 13X	1	0.27	20	10
PSA-7B	31-Jul	KB18	5A and 13X	1	0.27	17.1	10
PSA-8A	12-Aug	KA20	5A and 13X	1	Humid	5.1162	10
PSA-8B	12-Aug	KB22	5A and 13X	1	Humid	5.1162	10
PSA-9A	13-Aug	KB24	5A and 13X	1	Humid	5.097	10
PSA-9B	13-Aug	KB23	5A and 13X	1	Humid	5.097	10
PSA-10A	14-Aug	KB24	5A and 13X	1	Humid	7.566	10
PSA-10B	14-Aug	KB23	5A and 13X	1	Humid	7.566	10
PSA-11A	15-Aug	KB26	5A and 13X	1	Humid	8.592	10
PSA-11B	15-Aug	KB25	5A and 13X	1	Humid	8.592	10
PSA-12A	16-Aug	KB26	5A and 13X	1	Humid	10.158	10
PSA-12B	16-Aug	KB25	5A and 13X	1	Humid	10.158	10
PSA-13A	23-Aug	BD27	FCMS	0.96	Dry	3.7308	10
PSA-14A	23-Aug	BD27	FCMS	0.96	Dry	3.018	10

APPENDIX

TEST MATRIX, SECOND YEAR

Date	Test Ref.	Bed	Material	1/2 Cycle, min	Dew-point	Pressure, psia	Mass Flow, lb/hr	$PPCO_2$, % $PPCO_2$
16-Feb		Iso 3, side 2	X28	6	High	3.75	5.3	3.10
16-Feb		Iso 3, side 2	X28	6	High	3.75	2.6	3.10
17-Feb	60% face	Iso 4, side 2	X28	6	High	3.75	5.3	3.10
17-Feb	60% face	Iso 4, side 2	X28	6	High	3.75	2.6	3.10
19-Feb	50% length	Iso 5, side 2	X28	6	High	3.75	5.3	3.10
19-Feb	50% length	Iso 5, side 2	X28	6	High	3.75	2.6	3.10
26-Feb	Desorb at tank	Iso 6	X28	NA	High	3.75	2.6	3.10
27-Feb	High CO_2 conc	Iso 6	X28	6	High	3.75	5.3	3.10
27-Feb	High CO_2 conc	Iso 6	X28	6	High	3.75	2.6	3.10
28-Feb		Iso 6	X28	6	Dry	3.75	2.6	3.10
28-Feb		Iso 6	X28	6	Dry	3.75	2.6	3.10
4-Mar	Desorb, both sides	Iso 6	X28	6	High	3.75	5.3	3.10
5-Mar	Nitro-burst	Iso 6	X28	6	High	3.75	5.3	3.10
6-Mar	Nitro-stream	Iso 6	X28	6	High	3.75	5.3	3.10
12-Mar	Nitro-stream	Iso 6	X28	6	High	3.75	5.3	3.10
13-Mar	Hot H_2O	Iso 6	X28	6	High	3.75	5.3	3.10
14-Mar		TC 6	X28	6	High	3.75	5.3	3.10
17-Mar		TC 6	X28	12	High	3.75	2.6	3.10
18-Mar		TC 6	X28	6	High	3.75	2.6	3.10
26-Mar	Sat	TC 7	X28 & 28B	NA	High	14.7	3.35	0.26
1-Apr	Sat	TC 7	X28 & 28B	NA	High	14.7	3.35	0.51
3-Apr	Sat	TC 7	X28 & 28B	NA	High	14.7	5.93	0.26
7-Apr	Sat	TC 7	X28 & 28B	NA	High	14.7	5.93	0.51
7-Apr	Sat	TC 7	X28 & 28B	NA	High	14.7	11.87	0.26

APPENDIX

TEST MATRIX, SECOND YEAR
(Continued)

Date	Test Ref.	Bed	Material	1/2 Cycle, min	Dew-point	Pres-sure, psia	Mass Flow, lb/hr	PPCO$_2$, % PPCO$_2$
8-Apr	Sat	TC 7	X28 & 28B	NA	High	14.7	11.87	0.51
9-Apr	Low CO$_2$ CDRA	TC 7	X28 & 28B	60	High	14.7	3.35	0.26
10-Apr	Low CO$_2$ CDRA	TC 7	X28 & 28B	30	High	14.7	3.35	0.26
11-Apr	High CO$_2$ CDRA	TC 7	X28 & 28B	30	High	14.7	3.35	0.51
14-Apr	High CO$_2$ CDRA	TC 7	X28 & 28B	60	High	14.7	3.35	0.51
17-Apr	Low CO$_2$ CDRA	TC 7	X28 & 28B	30	High	14.7	3.35	0.51
18-Apr	High CO$_2$ CDRA	TC 7	X28 & 28B	30	High	14.7	3.35	0.26
21-Apr	Adiabatic	ADI 3	X28B	NA	High	14.7	3.35	0.51
22-Apr	Adiabatic	ADI 3	X28B	30	High	14.7	3.35	0.51
30-Apr	Station	TC 8	13x + 5A	NA	High	14.7	5	0.51
1-May	Station	TC 8	13x + 5A	NA	High	14.7	5	0.26
2-May	Station	TC 8	13x + 5A	10	High	14.7	5	0.51
6-May	Station	TC 8	13x + 5A	30	Dry	14.7	3.35	0.51
8-May	Station	TC 8	13x + 5A	30	High	14.7	3.35	0.51
12-May	Station	TC 8	13x + 5A	30	High	14.7	3.35	0.51
19-May	Suit	TC 8	13x + 5A	NA	Dry	3.75	5.3	0.31
20-May	Suit	TC 8	13x + 5A	6	Dry	3.75	5.3	3.10
21-May	Suit	TC 8	13x + 5A	NA	Dry	3.75	5.3	3.10
22-May	Suit	TC 8	13x + 5A	6	High	3.75	5.3	3.10
23-May	Suit	TC 9, side 2	13x + 5A	NA	High	3.75	5.3	3.10
3-Jun	Suit	TC 10, side 2	X28B	6	High	3.75	5.3	3.10
3-Jun	Suit	TC 10, side 2	X28B	6	High	3.75	5.3	3.10
4-Jun	Suit	TC 10, side 2	X28B	6	High	3.75	5.3	3.10
5-Jun	Station	TC 10, side 2	X28B	NA	High	14.7	3.35	0.40

REPORT DOCUMENTATION PAGE

Form Approved
OMB No. 0704-0188

1. AGENCY USE ONLY (Leave blank)	2. REPORT DATE September 1996	3. REPORT TYPE AND DATES COVERED Final Report

4. TITLE AND SUBTITLE
Enhanced Molecular Sieve CO_2 Removal Evaluation Final Report

5. FUNDING NUMBERS

6. AUTHOR(S)
El Sherif, Dina; MacKnight, Allen; Rose, Susan

7. PERFORMING ORGANIZATION NAME(S) AND ADDRESS(ES)
AlliedSignal Aerospace
2525 W. 190th Street
Torrance, CA 90509

8. PERFORMING ORGANIZATION REPORT NUMBER
97-69288

9. SPONSORING/MONITORING AGENCY NAME(S) AND ADDRESS(ES)
National Aeronautics and Space Administration
Washington, DC 20546

10. SPONSORING/MONITORING AGENCY REPORT NUMBER

11. SUPPLEMENTARY NOTES
Final Report

12a. DISTRIBUTION/AVAILABILITY STATEMENT
Unclassified — Unlimited

12B. DISTRIBUTION CODE

13. ABSTRACT (Maximum 200 words)

The objective of this research is to quantitatively characterize the performance of two major types of molecular sieves for two-bed regenerative carbon dioxide removal at the conditions compatible with both a spacesuit and station application. One sorbent is a zeolite-based molecular sieve that has been substantially improved over the materials used in Skylab. The second sorbent is a recently developed carbon-based molecular sieve. Both molecular sieves offer the potential of high payoff for future manned missions by reducing system complexity, weight (including consumables), and power consumption in comparison with competing concepts. The research reported here provides the technical data required to improve CO_2 removal systems for regenerative life support systems for future IVA and EVA missions.

14. SUBJECT TERMS
Advanced life support, carbon dioxide removal, air revitalization

15. NUMBER OF PAGES

16. PRICE CODE

17. SECURITY CLASSIFICATION OF REPORT	18. SECURITY CLASSIFICATION OF THIS PAGE	19. SECURITY CLASSIFICATION OF ABSTRACT	20. LIMITATION OF ABSTRACT
Unclassified	Unclassified	Unclassified	Unlimited

NSN 7540-01-280-5500

Standard Form 298 (Rev. 2/89)